Polymer Chemistry

Influence of an Ester Directing-Group on Defect Formation in the Synthesis of Conjugated Polymers via Direct Arylation Polymerization (DArP) using Sustainable Solvents

Journal:	*Polymer Chemistry*
Manuscript ID	PY-ART-06-2019-000815.R1
Article Type:	Paper
Date Submitted by the Author:	10-Jul-2019
Complete List of Authors:	Pankow, Robert; University of Southern California, Chemistry Ye, Liwei; University of Southern California, Chemistry Thompson, Barry; University of Southern California, Chemistry

ARTICLE

Influence of an Ester Directing-Group on Defect Formation in the Synthesis of Conjugated Polymers via Direct Arylation Polymerization (DArP) using Sustainable Solvents

Received 00th January 20xx,
Accepted 00th January 20xx

DOI: 10.1039/x0xx00000x

Robert M. Pankow[a], Liwei Ye[a], and Barry C. Thompson*[a]

Direct arylation polymerization (DArP) is a synthetic methodology that allows for the preparation of conjugated polymers via C-H activation, facilitating a streamlined synthetic pathway for accessing monomers, while providing a reduction in the number of synthetic steps, hazardous waste, and toxic reagents. Improving the aspects of sustainability by changing the solvent or transition metal catalyst to a more sustainable alternative has recently garnered attention, and constitutes great importance for establishing DArP as an appealing alternative to commonly employed polymerization methods. Interestingly, while directing-groups are often employed for various small-molecule C-H couplings, use of these moeities have remained relatively unexplored despite their potential to enhance the reactivity of a given monomer. Towards these ends, we explore the use of the sustainable solvents cyclopentyl methyl ether (CPME) and anisole for the synthesis of a diester functionalized bithiophene using DArP to afford the copolymer poly[5,5′-bis(2-butyloctyl)-(2,2′-bithiophene)-4,4′-dicarboxylate-alt-5,5′-2,2′-bithiophene] (PDCBT) with a molecular weight (Mn) of 13.8 kDa and a yield of 59%. However, we observe the likely presence of branching (β) defects through analysis of ^{1}H-NMR spectroscopy, GIXRD, and UV-vis absorption spectroscopy measurements. In order to determine if defect formation can be avoided, we study the occurance of defect formation as a function of the aryl spacer by employing the electron rich thieno[3,2-b]thiophene (PDCTT) and electron deficient 2,2′-bithiazole (PDCBTz). We find the optimal conditions provide PDCTT and PDCBTz with molecular weights of 26.4 and 4.9 kDa and yields of 90% and 46%, respectively, where PDCBTz was prone to form insoluble, branched polymer. This demonstrates that PDCBTz has a heightened reactivity towards defect formation, relative to PDCBT, while PDCTT does not, and indicates that such defect formation can be controlled through the appropriate selection of monomers. This study provides valuable insight regarding functional group tolerance and the capacity for esters to potentially function as directing-groups, leading to the undesired couplings of distal protons.

Introduction

Interest in conjugated polymers is ever increasing, due to the wide-range of potential applications these materials can be used for.[1,2] Primarily, their inclusion in organic electronic applications, such as light-emitting diodes, thin-film transistors, and photovoltaics is of considerable interest since they offer a low-cost alternative to their inorganic counterparts.[3–5] In particular, bulk-heterojunction polymer solar cells have experienced a renaissance of sorts due to the optimization of non-fullerene acceptors (NFA).[6–8] Power conversion efficiencies (PCE) in excess of 15% have been achieved in these devices, providing strong motivation to further advance this technology as a viable alternative energy source.[9,10] A polymer of interest in such solar cells is poly[5,5′-bis(2-butyloctyl)-(2,2′-bithiophene)-4,4′-dicarboxylate-alt-5,5′-2,2′-bithiophene] (PDCBT), which is shown in Scheme 1. This polymer has great potential, given its relative ease of synthesis (Scheme 2 and 3)

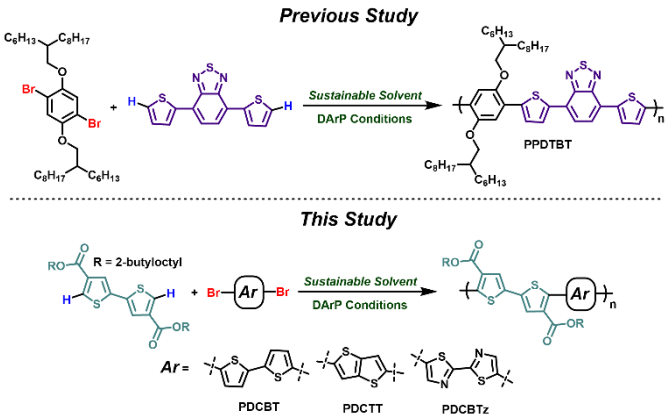

Scheme 1. Investigation of DArP using sustainable solvents towards the synthesis of PPDTBT (top), and the application of such solvents towards the synthesis of PDCBT, PDCBTT, and PDCBTz (bottom).

and the performance in both fullerene (PCE of >7%) and non-

[a] Department of Chemistry and Loker Hydrocarbon Research Institute, University of Southern California, Los Angeles, California 90089-1661. Email: barrycth@usc.edu
Electronic Supplementary Information (ESI) available: [Monomer synthesis and characterization, Polymer characterization]. See DOI: 10.1039/x0xx00000x

fullerene (PCE of >10%) solar cells is very desirable.[11–15]The short synthetic procedure for PDCBT, based on only a few steps from commercial starting materials, is consistent with scalability, a key guiding principle of sustainability in conjugated polymers.[16,17] Another guiding principle is the avoidance of highly hazardous reagents, e.g. pyrophoric or acute toxicants, However, the synthesis of PDCBT, and almost all conjugated polymers used in solar cells are still reliant on Migita-Stille (Stille) polymerizations, which invoke the use of an alkylstannane moiety for transmetallation, or Suzuki-Miyaura (Suzuki) polymerizations, which require the inclusion of an organoboronate on the monomer. This undermines the sustainability of conjugated polymers, through the use of highly hazardous reagents, cryogenic conditions, and a large accumulation of toxic byproducts.

In contrast, direct arylation polymerization (DArP) provides an avenue for conjugated polymer synthesis that is streamlined and sustainable, via the direct functionalization of C-H bonds during the polymerization.[18–24] Research efforts towards further improving the sustainability of DArP protocols has increased, with studies that investigate changing the solvent or transition metal catalyst to more sustainable alternatives.[25–28] This change to sustainable sources, be it the solvent or transition metal catalyst, present major challenges as the chemistry associated with the desired chemical transformation can be highly dependent on the solvent or catalyst employed.[29,30] To further develop and improve upon such changes, a paradigm shift has occurred within organic chemistry to develop more sustainable reaction conditions.[31–33] Extension of this field to conjugated polymer synthesis, or polymer synthesis in general, is not a straightforward pursuit, as mentioned above.[30,34] This is why the focus on this area has expanded, since there are many challenges still to be faced with regards to finding broadly applicable, truly sustainable conditions for conjugated polymer synthesis. Recently, we have reported DArP conditions using cyclopentyl methyl ether (CPME), which is a sustainable solvent allowing for the synthesis of conjugated polymers with a minimized environmental impact.[26] CPME is advantageous for large scale applications because it can be prepared in a waste-free process with starting materials sourced from biomass, it is not classified as a reproductive toxin or carcinogen, and it is not a peroxide former like 2-methyltetrahydrofuran (2-MeTHF).[35,36]

From our previous study, the reaction conditions using CPME required extended times (72 hours) compared to comparable DArP protocols (16 hours). In regards to donor-acceptor copolymer synthesis, only a single copolymer, poly[(2,5-bis(2-hexyldecyloxy)phenylene)-alt-(4,7-di(thiophen-2-yl)benzo[c][1,2,5]thiadiazole) (PPDTBT), which is shown in Scheme 1 (top), was reported. Furthermore, the sustainable solvent anisole, which can be derived from biomass, does not form peroxides, and has been utilized for the fabrication of polymer solar cells with good efficiencies (PCE > 11%), was not studied.[37–40] With this in mind, we were emboldened to explore improved reaction conditions with sustainable solvents and apply them to a broader scope of monomers that have not been studied with DArP.

Herein, we report the synthesis of PDCBT using the sustainable solvents CPME and anisole, with a goal of elucidating the influence of monomer structure, specifically an ester directing group, on the capacity for defect formation, which is described below. We find that the most effective conditions with CPME allow for the rapid synthesis of PDCBT in less than 1 hour (M_n =13.6 kDa and yield of 59%, shown in Table 1), which is a significantly lower reaction time than the previously reported for PPDTBT (reaction time of 72 hours).[26] It was observed, however, that gelation of the polymerization can occur leading to insoluble material if the timing of the reaction is further extended. This is believed to be potentially due to the formation of crosslinking or branching (β) defects, which has been observed for bithiophene based copolymers prepared via DArP.[41] Through analysis using GIXRD, UV-vis absorption spectroscopy, and ^{1}H-NMR spectroscopy we show that branching (β) defects are the likely cause of this gelation. We propose that activation of β-protons on the bithiophene comonomer and subsequent defect formation is likely enhanced by the coordinative and directing ability of the ester moiety on the acceptor unit of PDCBT.[42–44] While many studies have been conducted to determine the formation of defects with DArP, the effect of a directing-group, such as an ester, has not been accounted for or previously realized.[45]

In order to explore the impact of the ester directing groups on the adjacent β-protons, we applied the polymerization conditions used for PDCBT towards the synthesis of poly[5,5'-bis(2-butyloctyl)-(2,2'-bithiophene)-4,4'-dicarboxylate-alt-2,5-[3,2-b]thienothiophene] (PDCTT) and poly[5,5'-bis(2-butyloctyl)-(2,2'-bithiophene)-4,4'-dicarboxylate-alt-5,5'-2,2'-bithiazole] (PDCBTz), which are shown in Scheme 1. The thieno[3,2-b]thiophene (TT) and 2,2'bithiazole (BTz) provide simple model compounds to study how a more electron rich monomer or electron deficient monomer may inhibit or accelerate the formation of branching defects, respectively. We find that branching occurs excessively with PDCBTz, preventing the isolation of high M_n polymer, but not PDCTT. This investigation and the findings herein provide valuable insight regarding functional group tolerance for DArP.

Experimental

General Methods.

All reagents were purchased from VWR and used as received, unless otherwise noted. $Pd(PPh_3)_2Cl_2$ was purchased from Beantown Chemical and used as received. Pd_2dba_3 was purchased from Matrix Scientific and used as received. P(*o*-anisyl)$_3$ was purchased from TCI and used as received. Cs_2CO_3 and K_2CO_3 were ground to a fine powder and dried in a vacuum oven (120 °C) overnight then stored in a desiccator before use. Anhydrous cyclopentyl methyl ether (CPME) was purchased from Acros Organics and used as received. Compounds **2-12** were prepared following literature procedures. See ESI for complete synthetic details in regards to monomer synthesis. 5,5'-bis(trimethylstannyl)-2,2'-bithiophene (13) used for Stille polymerization was previously prepared following literature procedure.[46]

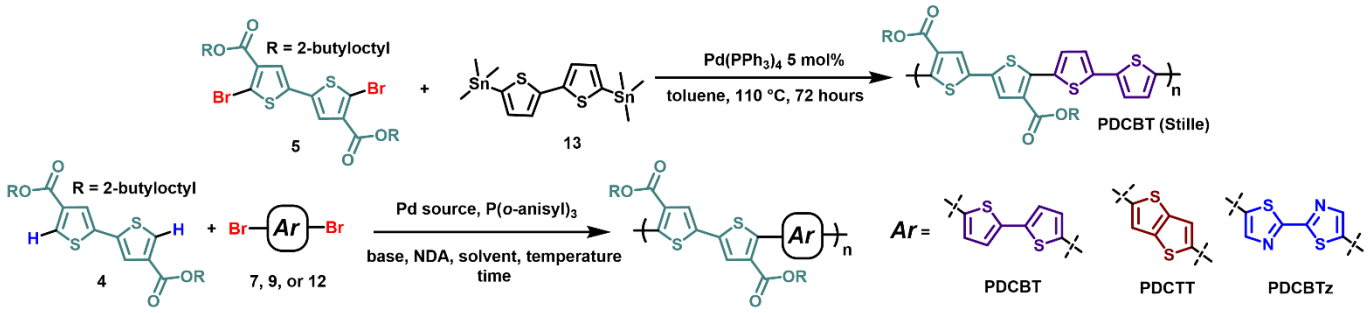

Scheme 2. Synthesis of PDCBT via Stille (top), and PDCBT, PDCTT, and PDCBTz via DArP (bottom).

Table 1 Detailed conditions and polymerization outcomes for the synthesis of PDCBT, PDCTT, and PDCBTz.

Entry	Polymer	Pd source[a]	Solvent (M)	Base (equiv.)	Temp. (°C)	Time (hours)	Yield (%)[b]	M_n (kDa)[b]	Đ[b]
1	PDCBT	Pd_2dba_3	THF (0.2)	Cs_2CO_3 (3)	120	16	NP	NP	NP
2	PDCBT	Pd_2dba_3	CPME (0.2)	Cs_2CO_3 (3.2)	110	16	72	7.9	2.08
3	PDCBT	$PdCl_2(PPh_3)_2$	CPME (0.2)	Cs_2CO_3 (3.2)	110	2	insoluble	insoluble	insoluble
4	PDCBT	$PdCl_2(PPh_3)_2$	CPME (0.2)	Cs_2CO_3 (3.2)	110	0.72	59	13.8	3.30
5[c]	PDCBT	$PdCl_2(PPh_3)_2$	CPME (0.2)	Cs_2CO_3 (2)	110	16	NP	NP	NP
6	PDCBT	$PdCl_2(PPh_3)_2$	CPME (0.2)	K_2CO_3 (3.2)	110	16	NP	NP	NP
7	PDCBT	$PdCl_2(PPh_3)_2$	Anisole (0.2)	Cs_2CO_3 (3.2)	110	16	77	8.3	2.13
8	PDCTT	$PdCl_2(PPh_3)_2$	CPME (0.2)	Cs_2CO_3 (3.2)	110	16	90	26.4	2.33
9	PDCBTz	$PdCl_2(PPh_3)_2$	CPME (0.2)	Cs_2CO_3 (3.2)	110	1.1	46	4.9	4.09
10	PDCBTz	$PdCl_2(PPh_3)_2$	CPME (0.2)	Cs_2CO_3 (3.2)	110	1	54	3.4	2.62
Stille	PDCBT	$Pd(PPh_3)_4$	Toluene (0.06)	-	110	72	95	24.0	3.08

[a]2 mol% loading for when Pd_2dba_3 is employed and 4 mol% for when $PdCl_2(PPh_3)_2$ is employed.[b] Determined after purification of the polymers via Soxhlet extraction. [c]Catalyst loading lowered from 4 mol% to 2 mol%. NP indicates an unsatisfactory or no precipitation from the reaction mixture prohibiting further purification.

All NMR were recorded at 25 °C using $CDCl_3$ on either a Varian Mercury 400 MHz, Varian VNMRS-500 MHz, or a Varian VNMR-600 MHz. All spectra were referenced to $CHCl_3$ (7.26 ppm), unless otherwise noted. Number average molecular weight (M_n) and polydispersity (Đ) were determined by size exclusion chromatography (SEC) using a Viscotek GPC Max VE 2001 separation module and a Viscotek Model 2501 UV detector, with 60 °C HPLC grade 1,2-dichlorobenzene (*o*-DCB) as

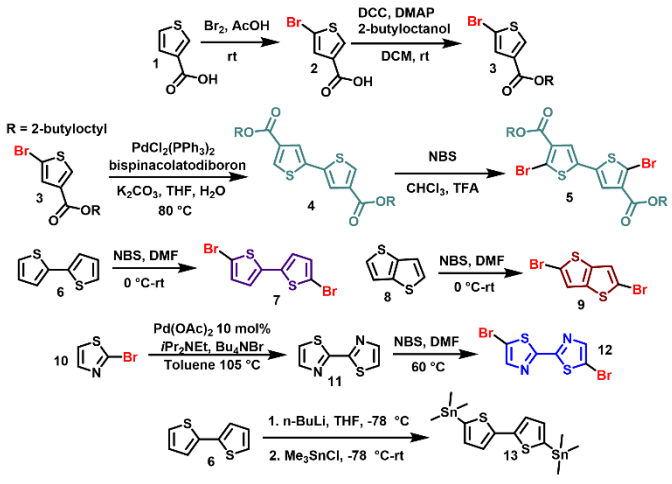

Scheme 3. Monomer synthesis.

eluent at a flow rate of 0.6 mL/min on one 300 × 7.8 mm TSK-Gel GMHHR-H column (Tosoh Corp). The instrument was calibrated vs. polystyrene standards (1050–3,800,000 g/mol), and data were analysed using OmniSec 4.6.0 software. Polymer samples were dissolved in HPLC grade o-dichlorobenzene at a concentration of 0.5 mg ml−1, stirred at 65 °C until dissolved, cooled to room temperature, and filtered through a 0.2 µm PTFE filter.

For polymer thin-film measurements, solutions were spin-coated onto pre-cleaned glass slides from chloroform solutions at 7 mg/mL, which were then annealed at 150 °C for 30 minutes under N_2. UV−vis absorption spectra were obtained on a Perkin-Elmer Lambda 950 spectrophotometer. Thicknesses of the samples and grazing incidence X-ray diffraction (GIXRD) measurements were obtained using Rigaku diffractometer Ultima IV using a Cu Kα radiation source (λ = 1.54 Å) in the reflectivity and grazing incidence X-ray diffraction mode, respectively. Crystallite size was estimated using Scherrer's equation, shown with equation 1:

$$\tau = K\lambda/(\beta \cos\theta) \quad (1)$$

where τ is the mean size of the ordered domains, K is the dimensionless shape factor (K = 0.9), λ is the x-ray wavelength, β is the line broadening at half the maximum intensity (FWHM) in radians, and θ is the Bragg angle.

Synthesis of PDCBT via Stille.

To a 3-neck round bottom flask equipped with a stir-bar, nitrogen inlet, glass-stopper, Teflon septum, condenser, and under an inert, nitrogen atmosphere was added 5,5'-bis(trimethylstannyl)-2,2'-bithiophene (104 mg, 0.14 mmol, 1 equiv.) and **5** (68.5 mg, 0.14 mmol, 1 equiv.). Toluene (4.5 mL) was then added and the mixture degassed with N_2 for 20 minutes. $Pd(PPh_3)_4$ (11 mg, 0.007 mmol, 5 mol%) was added quickly to the flask, and it was then degassed again for 20 minutes. The Teflon septum was replaced with a glass stopper,

and the mixture was then heated at 110 °C for 72 hours. $CHCl_3$ (5 mL) was added with gentle heating to dissolve the solids, and the mixture was precipitated into a chilled 10% NH_4OH/MeOH solution with high-stirring. The solids were then filtered into a Soxhlet thimble and purified via Soxhlet extraction (MeOH, hexanes, and $CHCl_3$). The $CHCl_3$ fraction was concentrated, transferred to a tared vial, the solvent stripped, and the polymer further dried overnight under vacuum (~100 mtorr). ^{1}H-NMR (500 MHz, $CDCl_3$): ^{1}H-NMR (500 MHz, $CDCl_3$): δ(ppm) 7.56-7.46 (br, 4H), 7.20 (br, 2H), 4.21 (d, *J* = 5.0 Hz, 4H), 1.75 (br, 2H), 1.32-1.28 (br, 32H), 0.91-0.86 (br, 12H). Consistent with literature reports.[47]

Synthesis of PDCBT via DArP (Entry 3 of Table 1)

An oven dried, high-pressure vessel (15 mL) was capped with an inverted red-rubber septum and cooled under a stream of nitrogen for 15 minutes. Compound 4 (100 mg, 0.17 mmol, 1 equiv.), neodecanoic acid (29 mg, 0.17 mmol, 1 equiv), 5,5′-dibromo-2,2′-bithiophene (55 mg, 0.17 mmol, 1 equiv.), P(*o*-anisyl)$_3$ (9.5 mg, 0.16 equiv), $PdCl_2(PPh_3)_2$ (4.77 mg, 0.0068 mmol, 0.04 equiv), and Cs_2CO_3 (180 mg, mmol, 3.2 equiv) was added. The vessel was then sparged with a stream of nitrogen for 10 minutes. CPME (1.7 mL), which was from a 5 mL stock that had been degassed prior with N_2 for 15 minutes, was quickly added and the rubber septum quickly replaced with a Teflon screwcap equipped with a rubber o-ring. The sealed vial was the placed into a preheated oil bath (110 °C) and stirred for 43 minutes. The vial was then removed from heat, $CHCl_3$ (5 mL) was added with gentle heating to dissolve the solids, and the mixture was precipitated into a chilled 10% NH_4OH/MeOH solution with high-stirring. The solids were then filtered into a Soxhlet thimble and purified via Soxhlet extraction (MeOH, hexanes, and $CHCl_3$). The $CHCl_3$ fraction was concentrated, transferred to a tared vial, the solvent stripped, and the polymer further dried overnight under vacuum (~100 mtorr). ^{1}H-NMR (500 MHz, $CDCl_3$): δ(ppm) 7.54-7.46 (br, 4H), 7.20 (br, 2H), 4.21 (d, *J* = 5.0 Hz, 4H), 1.75 (br, 2H), 1.32-1.28 (br, 32H), 0.91-0.86 (br, 12H). Consistent with literature reports.[47]

Synthesis of PDCTT via DArP (Entry 6 of Table 1).

Similar to that of PDCBT but with 5,5′-dibromo-2,2′-bithizaole (50.7 mg, 0.17 mmol, 1 equiv.) in place of 5,5′-dibromo-2,2′-bithiophene. ^{1}H-NMR (500 MHz, $CDCl_3$): δ(ppm) 7.76-7.57 (br, 4H), 4.19 (br, 4H), 1.76 (br, 2H), 1.29-0.79 (br, 44H). Consistent with literature reports.[47]

Synthesis of PDCBTz via DArP (Entry 7 of Table 1).

Similar to that of PDCBT but with 5,5′-dibromo-2,2′-bithizaole (55.4 mg, 0.17 mmol, 1 equiv.) in place of 5,5′-dibromo-2,2′-bithiophene. ^{1}H-NMR (600 MHz, $CDCl_3$): δ(ppm) 8.20-8.18 (br, 2H), 7.62-7.59 (br, 2H), 4.21 (br, 4H), 1.75 (br, 2H), 1.31-1.27 (br, 32H), 0.90-0.86 (br, 12H).

Results and Discussion

Polymer Synthesis of PDCBT via DArP

As depicted in **Scheme 3** (see ESI for complete details), the monomer syntheses follow similar routes to those found in the literature with the exception of compound **4**. It was found that the nickel-catalysed reductive homocoupling was low yielding (20-30%) in our hands, impeding the necessary scale-up to allow for the optimization of the polymerization step. Recently, Suzuki-Miyura conditions have been used for the preparation of similar compounds, albeit with simpler alkyl chains on the ester moiety, such as methyl or ethyl, and so these were successfully adapted to allow for a highly scalable synthesis of compound **4**. As reported by others, the bromination of compound **4**, which is required for Stille polymerization, proceeds with low levels of regio-selectivity leading to an inseparable byproduct if not performed carefully.[47] Due to these complications with the synthesis of monomer **5**, it was deemed that the donor should be halogenated for DArP studies considering that halogenation of the donor-units can proceed much more simply without harsh conditions, such as trifluoroacetic acid for a solvent. Furthermore, the high-pressure DArP conditions originally developed by Ozawa et al. and Leclerc et al., which we have demonstrated to be compatible with sustainable solvents, employ a halogenated donor-unit leaving the site for C-H activation on the acceptor-unit.[22,41] Thus, the functionalization pattern shown in Scheme 2, with the donor-unit being halogenated, was deemed the best route for polymer synthesis in general. Compounds **7**, **9**, and **12** were all prepared following their respective literature procedures.

As depicted in Scheme 2, with the results in Table 1 (Entry Stille), PDCBT was prepared via Stille polymerization following literature procedure with a M_n of 24 kDa in 95% yield.[11] An initial attempt for polymerization via DArP was performed using THF as a solvent, in order to see how polymerization proceeds using a more general and often applied set of conditions (Entry 1 of Table 1).[48,49] Interestingly, no polymer precipitate was formed after the reaction. This led us to conclude that the solvent, Pd-source, and temperature could be having an unforeseen, adverse effect on the synthesis of the polymer via DArP. Specifically, in regards to solvent, PDCBT prepared via Stille polymerization proceeds exclusively in toluene, directing us to believe that a more non-polar solvent may be beneficial. With this in mind, we chose CPME as the next solvent for study, given its development as a sustainable solvent for conjugated polymer synthesis and that it is less-polar than THF. As shown in Entry 2 of Table 1, changing the solvent from THF to CPME afforded polymer product in 72% yield with an M_n of 7.9 kDa.

As a next step, we chose to optimize the identity of the Pd-source, and we selected $PdCl_2(PPh_3)_2$ since it has been shown to provide an effective catalyst for DArP and other cross-coupling methodologies.[41,50–52] With the changes in solvent and Pd-source, we found that the polymerization mixture completely gelled in 2 hours, to yield a polymer product that was prohibitively insoluble (Entry 3 of Table 1). Specifically, the material isolated from the polymerization could not be isolated from the $CHCl_3$ or chlorobenzene (CB) Soxhlet fractions. This insolubility could be from achievement of a very high-M_n polymer product or from the introduction of defects due to undesired couplings, such as donor-donor homocouplings or branching (β) defects.[24,41,53] The cause of this observed catalyst dependence, can likely be traced to the higher reactivity for

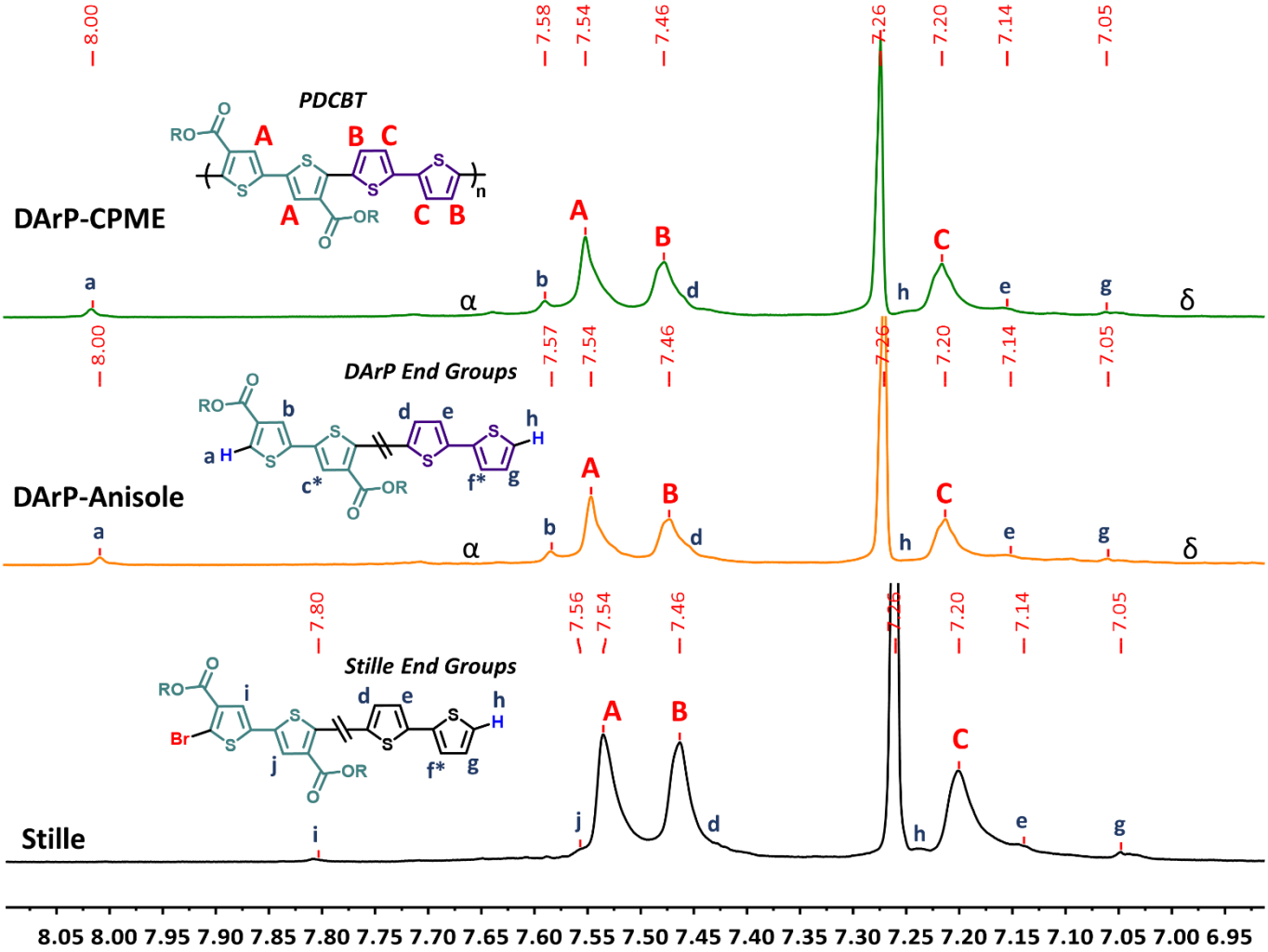

Figure 1. 1H-NMR ($CDCl_3$, 25 °C) of PDCBT prepared via DArP using the conditions outlined in Table 1: entry 4 (top), entry 7 (middle), and the Stille reference (bottom). End-group assignments are denoted by the lowercase letters (a-n) and the major resonances by the uppercase (A-C). For polymers prepared via DArP, acceptor-acceptor and donor-donor homocouplings are denoted by the characters, α and δ, respectively. Resonance labels with an asterisk (*) are not distinctly observed due to potential overlap (f* at 7.26 and c* at 7.55 ppm). All spectra referenced to $CHCl_3$ at 7.26 ppm.

$PdCl_2(PPh3)_2$ in certain cross-coupling reactions and within DArP for certain monomers. Specifically, Leclerc et al. have reported conditions for the polymerization of substituted bithiophene based monomers using $PdCl_2(PPh_3)_2$ with P(o-anisyl)$_3$, achieving M_n of 52 kDa and a yield of 90%.[41] The results presented here as well as those described by Leclerc et al, indicate a preference for $PdCl_2(PPh_3)_2$ over Pd_2dba_3 when using bithiophene based monomers (Entries 2 and 4 of Table 1, respectively). Based on previous studies, $PdCl_2(PPh_3)_2$ has been shown to form anionic species ($Pd^0(L)_2(X)^{-1}$) from the highly reactive intermediate $Pd^0(L)_2$, both of which exhibit faster rates of oxidative addition than the $Pd^0(L)_4$ likely formed from Pd_2dba_3.[52,54] Formation of such a species, however, requires the in situ reduction of the Pd^{II}-precatalyst ($PdCl_2(PPh_3)_2$), which may only be a favorable process for only certain monomers, such as functionalized bithiophenes.[55] Furthermore, the dba ligand (from Pd_2dba_3) has been reported to stabilize the Pd^0 species to the point that it impedes catalysis or that it can interfere with the desired catalytic transformation, which may be occurring with the polymerizations described here.[55,56] While such reactivity is dependent on the monomers under study, such a heightened reactivity for $PdCl_2(PPh)_3$ is interesting given the prevalence of Pd_2dba_3 in donor-acceptor copolymer synthesis via DArP. To see if a soluble polymer product could be obtained that would allow for structural characterization, the reaction time was shortened and the polymerization was closely monitored so that it can be stopped just at the onset of gelation, where the polymerization changes from a red to violet-red color. It was found that after 43 minutes, or 0.72 hours, the onset of gelation occurs and a polymer product that exhibits good solubility (allowing for complete purification and isolation via Soxhlet extraction) is obtained (Entry 4 of Table 1) with a satisfactory M_n (13.8 kDa) and yield (59%). These conditions provide significant improvement from the original high-pressure THF based conditions originally used (no polymer product after 16 hours), and also the polymerizations reported in our previous study, where 72 hours was required to provide optimal results with CPME.[26] Additional efforts were made to control the observed high reactivity, by lowering the equivalents of Cs_2CO_3 from 3.2 to 2.0 and the catalyst loading

from 4 mol% to 2 mol% (Entry 5 of Table 1) and changing the base to K_2CO_3 (Entry 6 of Table 1). However, these changes did not provide a satisfactory polymer precipitate from their respective reaction mixtures. With regards to changing the equivalents of base (Entry 5), the result of no polymer product forming is likely due to only 1 equivalent of reactive base (Cs_2CO_3) being present, with the remainder being quenched to $CsHCO_3$, as previously discussed by Ozawa et al.[22,57] Although the catalyst loading has been lowered, going from 4 to 2 mol% will likely not have as detrimental of effect as lowering the base. This is because many DArP protocols, using similar conditions, use a catalyst loading of 1 to 2 mol%. In our previous study regarding sustainable solvents, we found that lowering the catalyst loading from 4 to 1 mol% actually led to an increase in Mn (from 31 to 41 kDa) for PPDTBT.[26] Furthermore, Leclerc's study regarding the DArP of dialkyl bithiophenes shows that the inherent reactivity of the monomer protons, such as the α or β protons, is what determines the propensity for defect formation for a given condition set, which is further discussed below.[41] Therefore, monomers with a greater potential for defect formation, such as those with an ester directing group, should be tailored or functionalized so as to prohibit the undesired activation of branching sites, since the tuning of reaction conditions, such as equivalents or identity of base and loading of catalyst, cannot necessarily allow for the exclusion of defects.

We were then interested to see the effect of changing the solvent, specifically with anisole. Anisole is less polar than THF with a dielectric constant of 4.33 versus 7.58 and, as described earlier, can be used as a more sustainable solvent for conjugated polymer synthesis and processing.[39,58,59] The dielectric constant is closer to that of CPME as well, which is at 4.76.[36] Interestingly, anisole was found to slow the rate of polymerization, by observation, since no gelation was observed (Entry 7 of Table 1). Consequentially, this led to a polymer with lower M_n (8.3 kDa), but an improved yield (77%). The dependence of the reaction on the choice of solvent is difficult to determine given the critical role of the solvent within this type of transformation, e.g. solubility of the base, coordination to palladium, and potential activation of halogens.[52,60,61] Given this, it is possible that the slight increase in polarity for CPME over anisole (4.76 versus 4.33, respectively) may help to stabilize transition states, intermediates, or provide improved solubility of the growing polymer chain. It is likely that through more extensive optimization or with a different copolymer the reaction time and outcome of the polymerization using anisole can be improved, and so anisole should not be discounted as a sustainable solvent for DArP.

^{1}H-NMR Characterization of DArP-PDCBT

To determine if the structure of the DArP-synthesized polymers match that of the known Stille synthesized PDCBT, ^{1}H-NMR spectroscopy was used, which is shown in Figure 1. The polymers, both those prepared using DArP and Stille, exhibited excellent solubility in chloroform allowing for well-defined resonances to be obtained in the spectra. As shown in Figure 1 (bottom spectrum), the Stille polymer shows three well defined resonances centered at 7.54, 7.46, and 7.20 ppm (A-C). These are in agreement with the observed literature values.[11,47] End-group assignments are based on the observed resonances for monomers and model compounds collected in $CDCl_3$ with identical or similar structure.[11,47,62] Interestingly, end-groups associated with destannylated bithiophene are observed at 7.25 ppm (label h, Figure 1). This is likely due to destannylation, which has been observed for electron-rich heterocyclic stannanes.[63]

For the polymers prepared via DArP (Figure 1, top and middle), the major resonances (A, B, and C) align very well with the Stille-reference polymer. Also, the smaller, distinct resonances (a-h, Figure 1) can be assigned to the expected end-groups of either the ester functionalized bithiophene or bithiophene, indicating good structural fidelity for the DArP polymers. Importantly, acceptor-acceptor homocoupling peaks (α), which can occur via an oxidative coupling and has been reported for monomers of similar structure, e.g. ester-functionalized thiophenes, are not observed at 7.66 ppm (Figure 1, top and middle).[50,64] An expanded view of this region (7.75-7.60 ppm) in the ESI (Figure S13), shows that acceptor-acceptor homocouplings are not present and that the small resonances near this point are also in the Stille-PDCBT. These smaller resonances present in both DArP-PDCBT and Stille-PDCBT likely correspond to the penultimate protons near the terminus of the polymer. Also, donor-donor homocouplings (δ) are not observed at 6.98 ppm.[65] End-groups corresponding to the bithiophene end-group are easily apparent (d-h, Figure 1). As with the Stille-reference, resonances corresponding to f* are not observed, likely due to overlap with the major resonance from solvent ($CHCl_3$) at 7.26 ppm. Shoulders near 7.45 ppm corresponding to proton d, are better defined in the DArP PDCBT polymers, compared with the Stille-reference. These results indicate that the conditions employed for entry 4 and 7 of Table 1 provide polymer product with good structural fidelity with regards to an absence of α and δ homocouplings, as observed by ^{1}H-NMR. Of the two homocoupling defects, δ homocouplings would be the likely cause of insoluble material to form, since no solubilizing alkyl chains are present on the bithiophene donor. Given their absence, in the case of Entry 4, this indicates that gelation and formation of insoluble material is likely occurring through crosslinking or β-defect formation, although these structural features are challenging to observe via ^{1}H-NMR.[24,41,66,67]

This conclusion on potential β-defect formation for PDCBT is reached based on previous DArP studies we have performed, which describe the defect free synthesis of P3HT and PPDTBT using similar conditions (Figure 2a).[26,68] Similar conditions were also applied towards the synthesis of PPDBTTPD (Figure 2a), which possesses numerous, unobstructed β-protons.[49] In each of these studies, no prohibitively insoluble material was obtained (even when precipitation during the polymerization was observed), and thorough characterization of these polymers confirmed an absence of β-defects. In the case of the aforementioned polymers (P3HT, PPDTBT, and PPDBTTPD), neodecanoic acid (NDA) inhibits β-defect formation by sterically shielding the β-protons ($H\beta_1$-$H\beta_4$) from the Pd-catalyst.[69] Since NDA is present (1 equiv.) in the DArP conditions reported here,

β-defect formation must either be overcoming the steric hindrance or displacement of the NDA coordinated to Pd by the ester moiety is occurring. Esters, specifically, have been shown by Yu et al. to allow for the C-H activation of distal protons, via

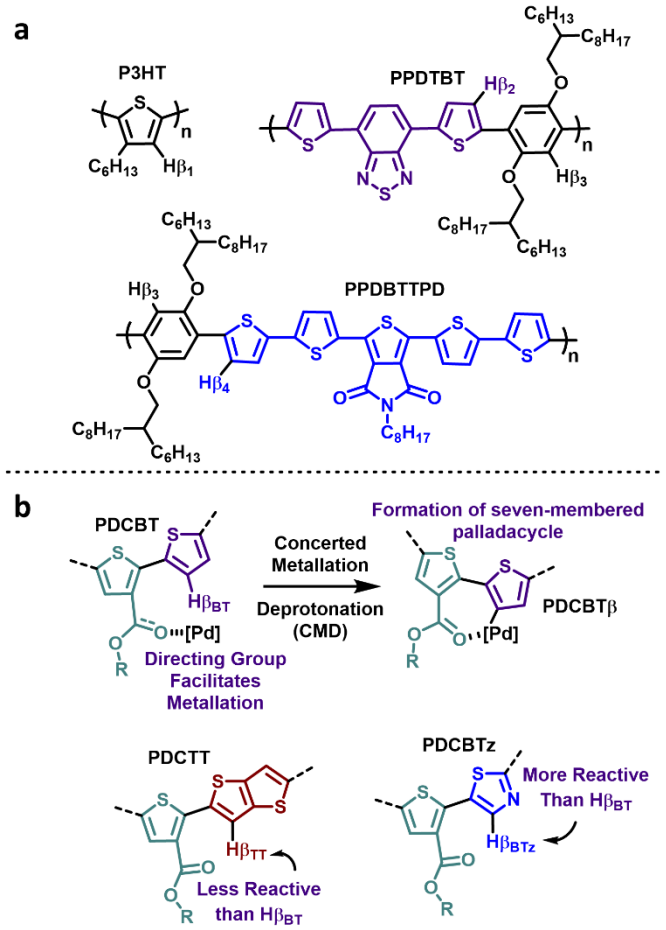

Figure 2. (a) Polymers (P3HT and PPDTBT) for which the DArP conditions were optimized allowing for the exclusion of defects (α, β, and δ), allowing for the application of these conditions to polymers with a greater potential for β-defect formation (PPDBTTPD). (b) Depiction of the directing group effect of the ester on PDCBT forming PDCBTβ, and the suppression or enhancement for β-defect formation when biaryls with different β-protons (PDCTT and PDCBTz) are used compared with PDCBT.

a seven-membered cyclopalladation, on electron rich arenes.[43] In the aforementioned study, the ester moiety displaced the carboxylic acid ligand used, allowing for C-H functionalization to occur. This type of reactivity is analogous to what we propose for PDCBT. Specifically, the ester directing group likely displaces the NDA and then the palladium metal center can form a seven-membered palladacycle with the adjacent thiophene aryl group (Figure 2b), which is based on the findings by Yu's aforementioned study. While directing groups (not carbonyl based) have been used in the synthesis of conjugated polymers via DArP, this mechanism of defect formation has not been explicitly observed to our knowledge.[70]

Synthesis of PDCTT and PDCBTz via DArP

As mentioned prior, the primary method for preventing β-defect formation in DArP is the use of a bulky carboxylic acid, such as NDA, but if carbonyl groups along the backbone can displace NDA then defect formation can occur. Applying the conditions then to a more reactive (BTz) and less reactive (TT) monomer would offer insight regarding how β-proton reactivity effects the propensity for defect formation (Figure 2b). Using these monomers for their respective copolymer synthesis, we expect to see an enhanced or uncontrollable level of defects with BTz and a suppression of such defects with TT relative to BT.

Describing BTz and TT as more and less reactive towards β-defect formation is based on previous studies in DArP and small-molecule C-H activation. Specifically, based on the previous studies by Leclerc et al. regarding the Gibbs free energy ($\Delta G^{\ddagger}_{298K}$) associated with C-H bond cleavage at the concerted metalation deprotonation (CMD) transition state (TS), the reactivity of β-protons for BTz ($\Delta G^{\ddagger}_{298K}$ = 26.7 kcal) should be greater than that of BT ($\Delta G^{\ddagger}_{298K}$ = 28.3 kcal).[41,71] This type of calculation has not been performed for TT. However, low-reactivity for TT has been observed, where no polymerization proceeded via DArP unless a substituted TT was used to enhance its reactivity.[72] Furthermore, previous studies regarding the C-H activation of thieno[3,2-b]thiophene have concluded that Pd-catalysed oxidative conditions, which differ greatly from the ones employed here, are required for activation of the $H_{\beta TT}$ proton (Figure 2b), and that conditions reliant on the pKa of the proton, such as the ones employed for this study, do not provide coupled products in $H_{\beta TT}$ position.[73–75] In addition to a diminished reactivity, studies on the conformation of a TT unit flanked by carboxylate containing thiophenes, such as with PDCBT and PDCTT, have shown that twisting along the conjugated backbone occurs in the case of TT where BT is considered to be coplanar.[76] This twisting, which may be due to steric congestion brought upon by the more compact structure of the TT ring, leads to a large dihedral angle (>60°), which may inhibit formation of the seven-membered palladacycle intermediate (PDCBTβ, Figure 2b). Since BTz is structurally and spatially similar to BT, it is presumed that backbone twisting will not occur and that it should possess a nearly coplanar conformation as with PDCBT.

Confirming the ideas above, when the DArP conditions (Entry 4 of Table 1) that led to gelation with PDCBT were applied to PDCTT, we found that the polymerization mixture did not gel after 2 hours (Entry 8 of Table 1), and so the polymerization was left to go overnight (16 hours). After purification, it was found that the PDCTT obtained from this reaction provided a greater M_n (26 kDa) and yield (90%), relative to the same conditions for PDCBT. It should be noted that no $CHCl_3$-insoluble material was left-over after Soxhlet purification. It is likely that the extended reaction time contributes to the increase in yield and M_n, relative to PDCBT.[47] These results demonstrate that a monomer relatively with inert β-protons, compared to BT, can be employed when directing groups are present within the copolymer to successfully afford the desired copolymer.

When 2,2'-bithiazole was used, a reactivity for this monomer like that of bithiophene was observed. Specifically, onset of gelation of the reaction mixture was observed after 70 minutes leading to oligomeric material (M_n of 4.9 kDa with a yield of 46%) that could be isolated in the $CHCl_3$ fraction of the

Soxhlet (Entry 9 of Table 1), but with a small portion that was prohibitively insoluble in the chloroform fraction of the Soxhlet. In order to see if a more soluble polymer product could be isolated with a decreased reaction time, as was observed with PDCBT, the polymerization was repeated but was stopped at 60 minutes (Entry 10 of Table 1). This afforded an oligomeric product that was entirely soluble in the $CHCl_3$ fraction of the Soxhlet (M_n of 3.4 kDa and 54% yield) with an improved yield albeit lower molecular weight. Based on these results, it is clear that the reaction conditions, which affords isolable polymer products for PDCBT and PDCTT with good molecular weights and yields, are not optimal or controllable for a more electron deficient monomer prone to activation of the β-proton, such as bithiazole. C-H activation of this proton ($H\beta_{BTz}$, Figure 2b) is

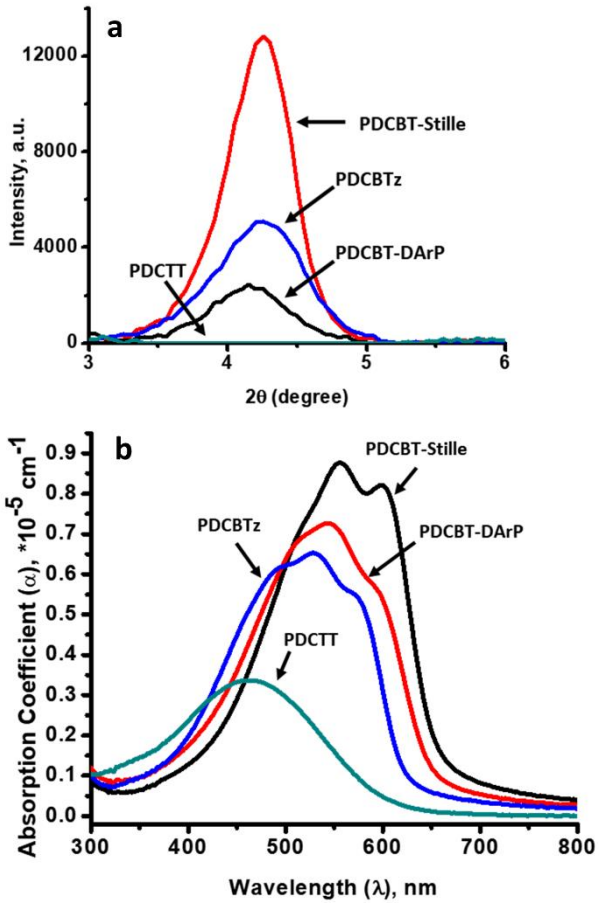

Figure 3. (a) GIXRD diffraction patterns for the polymers PDCBT-Stille, PDCBT-DArP, PDCTT, and PDCBTz. (b) Absorption profiles for the polymers PDCBT-Stille, PDCBT-DArP, PDCTT, and PDCBTz.

presumed to be highly favourable, and as the concentration of the monomers decreases in the reaction mixture defect formation, such as crosslinking and branching, will likely become more favourable. This would make cross-linking or β-couplings highly competitive relative to the desired coupling for PDCBTz, leading to insoluble materials before polymer products of desirable molecular weights and yields can be obtained, as with PDCTT.

Although somewhat intuitive, this correlation between structure and reactivity provides a general guide for in applying this methodology towards the synthesis of other copolymers. Specifically, electron deficient monomers used in concert with directing groups may invoke undesired couplings when protons that can undergo C-H activation are within a reasonable proximity. Based on these results, it is presumed that this type of directing group effect is possible with PDCBT, causing the activation of undesired protons and leading to the observed gelation during the polymerization. The NMR spectra for all of the synthesized polymers is provided in the ESI and referenced to polymers of known structure, but ^{1}H-NMR is not a general method for determining the presence of β-defects. Therefore, we confirm their presence using GIXRD and UV-vis absorption spectroscopy.

GIXRD and UV-vis Characterization of Polymer Films

The inclusion of β-defects within a conjugated polymer backbone has pronounced effects on the thin-film structural and electronic properties. As a consequence of the disorder caused by the β-defect, coherent, periodic structure can be disrupted since ideal alignment of the polymer chains is inhibited by the inclusion of a defect. This can be observed, as mentioned previously, using GIXRD and UV-vis absorption spectroscopy. With P3HT (Figure 2a) prepared via DArP as an example, β-defect content as little as 0.16% can shift d_{100}-spacing by 0.5 Å and noticeably decrease the intensity of the vibronic shoulder and the magnitude of the absorption coefficient in the UV-vis absorption spectrum in comparison to Stille-P3HT.[67] A similar trend is expected for the polymer PDCBT prepared via DArP, which is expected to contain β-defects.

As depicted in Figure 3 and shown in Table 2, the semi crystallinity and photophysical properties of the polymer thin-

Table 2. GIXRD and UV-vis absorbance data for PDCBT, PDCTT, and PDCBTz. [a]Measured on polymer films prepared from a 7 mg/mL chloroform solution and annealed at 150 °C for 30 minutes

Entry (Polymer)	Conditions Used (Table 1)	λ_{max} (nm)[a]; α (cm^{-1})[a]	d_{100} (Å)[a]	Crystallite Size (nm)[a]
1 (PDCBT)	Stille	556; 88×10^3	20.8	15.0
2 (PDCBT)	Entry 4	543; 73×10^3	21.3	13.4
3 (PDCTT)	Entry 8	463; 34×10^3	-	-
4 (PDCBTz)	Entry 9	529; 65×10^3	20.8	11.5

films vary, which can be attributed to differences in the polymer structure, molecular weights (M_n), and inclusion of β-defects. Specifically, the PDCBT prepared via Stille (Entry 1 of Table 2), which has a M_n of 26 kDa (Table 1) possess a peak absorption (λ_{max}) at 556 nm and an absorption coefficient (α) of 88×10^3 cm^{-1} (Figure 3b), while that prepared via the optimal DArP conditions (Entry 4 of Table 1), which has a M_n approximately half that of the Stille polymer at 13.8 kDa displays a blue shifted λ_{max} at 543 nm and an α of 73×10^3 cm^{-1} (Entry 2 of Table 2). In regards to semicrystallinity (Table 2 and Figure 3a), the difference between the DArP and Stille PDCBT polymers is clear, with a lower degree of crystallinity and crystallite size (13.4 versus 15.0 nm, respectively) for the PDCBT prepared via DArP. The d_{100}-spacing (21.3 and 20.8 Å, respectively) for these polymers is also different by 0.5 Å (Table 2 Entries 1 and 2). Taken as whole, the diminished intensity of the vibronic

shoulder, the reduced absorption coefficient, and the increase in d_{100}-spacing provide significant evidence for β-defect formation.[67] While differences in polymer M_n could have an effect on the aborption profile, the differences are more likely ascribed to β-defect formation, since the M_n is greater than 10 kDa for the DArP-PDCBT (where polythiophenes are known to show saturation of their optical properties).[77] This conclusion is also based on our past observations with DArP and Stille-P3HT, as well PPDTBT (Figure 2a).[67,68]

In comparison to PDCBT, PDCTT (Entry 3 of Table 2) presents a rather featureless absorption profile (Figure 3b) with a blue shifted λ_{max} at 463 nm, similar to what has been previously reported (λ_{max} at 476 nm).[47] A vibronic shoulder was not expected with PDCTT since previous reports for this polymer depict a featureless absorption profile for the polymer prepared via Stille.[47] As discussed above, the diminished value for α (34×10^3 cm^{-1}) indicates a more disordered structure for this polymer, where orbital overlap of the π-system along the polymer backbone and the π-π interactions between polymer chains may be hindered due to twisting caused by steric-hindrance between the alkyl chains on the accepter unit.[76]Also, no diffraction was observed in the GIXRD measurements for this polymer further. As shown with previous studies, this is likely because temperatures in excess of 150 °C will be needed to induce crystallization and aggregation.[47,78] However, optimization of the thin-film morphology is not a focus of this study. Given that gelation did not occur with PDCTT and no insoluble material was observed after Soxhlet with $CHCl_3$, it is believed that presence of β-defects is highly minimized, if not excluded, for this polymer.

PDCBTz (Entry 4 of Table 2) shows an absorption profile similar to that of PDCBT (Figure 3b), with the appearance of a weak vibronic-shoulder and a λ_{max} at 529 nm (Figure 3b). It is notable that despite the more-electron deficient bithiazole unit being employed for this polymer, the blue shift for the polymer is rather slight (14 nm) versus the 80 nm observed for PDCTT. This provides further indication of how the donor unit for this class of polymers influences the planarity and orbital overlap of the π-system along the polymer backbone and the π-π interactions between polymer chains. In regards to semicrystallinity, PDCBTz (Entry 4 of Table 2) has a lamellar spacing of 20.8 Å, which is identical to the Stille-PDCBT polymer. However, the reduction in crystallite size, coupled with the weak vibronic shoulder in the UV-vis spectrum (Figure 3b), indicates that the PDCBTz isolated via DArP contains β-defects as was observed for PDCBT. These results provides evidence for the hypothesis that branching or cross-linking can be controlled by employing an electron-rich monomer that is more resilient against crosslinking or β-defect formation, such as TT. As described above, β-defect formation is supported when all the factors are taken into account. Specifically, in the synthesis of PDCBT and PDCBTz via DArP (see Table 2 for conditions) both lead to insoluble material, which is a major indication of a polymer laced with defects. ^{1}H-NMR confirms that δ-homocouplings, which could lead to insoluble material, are not occurring. GIXRD shows a reduction in the degree of crystallinity and a shift in the d-spacing consistent with β-defect formation. The UV-vis absorption profiles also show a reduction in the vibronic shoulder and the absorption coefficient. All of these pieces of evidence point to the likelihood of β-defect formation for the polymers PDCBT and PDCBTz, which leads to the formation of insoluble material during the polymerization.

Conclusions

In this study we presented the application of the sustainable solvents CPME and anisole towards the synthesis of PDCBT and its analogues, PDCTT and PDCBTz, via DArP. We find the diester moieties on the acceptor unit can function as directing groups enhancing the reactivity of the monomer designated for C-H bond functionalization providing a significant reduction in the polymerization time. This enhancement in reactivity comes at the cost of selectivity, however, since crosslinking or β-defect formation occurs leading to the formation of insoluble polymer products. This likely occurs through displacement of the NDA, which is used to suppress β-defect formation, from the palladium catalyst by the ester. Through careful optimization, we were able to develop DArP conditions that allowed for the synthesis of isolable PDCBT in less than one hour, when CPME is used as the solvent, with a molecular weight (M_n) of 13.8 kDa and a yield of 59%. Application of the optimal conditions towards the relatively electron rich, PDCTT, which contains thieno[3,2-b]thiophene, and electron deficient, PDCBTz, which contains 2,2'-bithiazole, was performed to investigate the occurrence of defect formation by varying the aryl group. Specifically, electron deficient monomers may invoke cross-linking or branching defects due to the higher reactivity of the protons in the conjugated backbone of the polymer, which was observed with PDCBTz. However, with the electron-rich PDCTT a polymer product with a M_n of 26 kDa and a yield of 90% was obtained. Characterization using GIXRD and UV-vis absorption spectroscopy confirmed the presence of β-defects in PDCBT and PDCBTz prepared via DArP. This demonstrates an important need for understanding functional group tolerance and a guiding principle when developing conditions for DArP. Based on our results, a directing group can facilitate C-H activation of distal protons on adjacent aryl groups forming undesired defects, despite use of a bulky carboxylic acid ligand (NDA). Suppression of such defects is possible through the judicious selection of a comonomer, which contains a β-proton of low reactivity or can inhibit the formation of the intermediate metallocycle. Future work will focus on determining conditions that allow for the defect-free synthesis of electron deficient of conjugated copolymers, such as PDCBTz, using sustainable solvents, and determine conditions that allow for a more controlled synthesis when directing groups are employed.

Conflicts of interest

There are no conflicts to declare.

Acknowledgements

This work was supported by the National Science Foundation (MSN under award number CHE-1608891) and the Dornsife/Graduate School Fellowship (to R.M.P).

References

‡ 1 Oksana. Ostroverkhova, *Chem. Rev. (Washington, DC, U. S.)*, 2016, **116**, 13279–13412.
2 S. Inal, J. Rivnay, A.-O. Suiu, G. G. Malliaras and I. McCulloch, *Acc. Chem. Res.*, 2018, **51**, 1368–1376.
3 A. N. Sokolov, B. C.-K. Tee, C. J. Bettinger, J. B.-H. Tok and Zhenan. Bao, *Acc. Chem. Res.*, 2012, **45**, 361–371.
4 A. C. Grimsdale, K. Leok Chan, R. E. Martin, P. G. Jokisz and A. B. Holmes, *Chem. Rev.*, 2009, **109**, 897–1091.
5 B. C. Thompson and J. M. J. Frechet, *Angew. Chem., Int. Ed.*, 2008, **47**, 58–77.
6 Y. Lin, J. Wang, Z.-G. Zhang, H. Bai, Y. Li, D. Zhu and X. Zhan, *Adv. Mater.*, 2015, **27**, 1170–1174.
7 A. Wadsworth, M. Moser, A. Marks, M. S. Little, N. Gasparini, C. J. Brabec, D. Baran and I. McCulloch, *Chem. Soc. Rev.*, 2019, **48**, 1596–1625.
8 Y. Cai, L. Huo and Y. Sun, *Advanced Materials*, 2017, **29**, 1605437.
9 J. Yuan, Y. Zhang, L. Zhou, G. Zhang, H.-L. Yip, T.-K. Lau, X. Lu, C. Zhu, H. Peng, P. A. Johnson, M. Leclerc, Y. Cao, J. Ulanski, Y. Li and Y. Zou, *Joule*, 2019, **3**, 1140-1151.
10 H. Yao, Y. Cui, D. Qian, C. S. Ponseca, A. Honarfar, Y. Xu, J. Xin, Z. Chen, L. Hong, B. Gao, R. Yu, Y. Zu, W. Ma, P. Chabera, T. Pullerits, A. Yartsev, F. Gao and J. Hou, *J. Am. Chem. Soc.*, 2019, **141**, 7743-7750.
11 M. Zhang, X. Guo, W. Ma, H. Ade and J. Hou, *Adv. Mater.*, 2014, **26**, 5880–5885.
12 M. Chang, Y. Wang, Y.-Q.-Q. Yi, X. Ke, X. Wan, C. Li and Y. Chen, *J. Mater. Chem. A*, 2018, **6**, 8586–8594.
13 H. Feng, Y.-Q.-Q. Yi, X. Ke, Y. Zhang, X. Wan, C. Li and Y. Chen, *Solar RRL*, 2018, **2**, 1800053.
14 Y. Liu, L. Zuo, X. Shi, A. K.-Y. Jen and D. S. Ginger, *ACS Energy Lett.*, 2018, **3**, 2396-2403.
15 Y. Qin, M. A. Uddin, Y. Chen, B. Jang, K. Zhao, Z. Zheng, R. Yu, T. J. Shin, H. Y. Woo and J. Hou, *Advanced Materials*, 2016, **28**, 9416–9422.
16 J. E. Carlé, M. Helgesen, O. Hagemann, M. Hösel, I. M. Heckler, E. Bundgaard, S. A. Gevorgyan, R. R. Søndergaard, M. Jørgensen, R. García-Valverde, S. Chaouki-Almagro, J. A. Villarejo and F. C. Krebs, *Joule*, 2017, **1**, 274–289.
17 N. S. Gobalasingham, J. E. Carle, F. C. Krebs, B. C. Thompson, E. Bundgaard and Martin. Helgesen, *Macromol. Rapid Commun.*, 2017, **38**, 1700526.
18 P.-O. Morin, T. Bura and M. Leclerc, *Mater. Horiz.*, 2015, **3**, 11–20.
19 N. S. Gobalasingham and B. C. Thompson, *Progress in Polymer Science*, 2018, **83**, 135–201.
20 H. Bohra and M. Wang, *Journal of Materials Chemistry A*, 2017, **5**, 11550–11571.
21 K. Okamoto, J. Zhang, J. B. Housekeeper, S. R. Marder and C. K. Luscombe, *Macromolecules*, 2013, **46**, 8059–8078.
22 M. Wakioka, Y. Kitano and F. Ozawa, *Macromolecules*, 2013, **46**, 370–374.
23 Y. Fujinami, J. Kuwabara, W. Lu, H. Hayashi and T. Kanbara, *ACS Macro Lett.*, 2012, **1**, 67–70.
24 F. Lombeck, F. Marx, K. Strassel, S. Kunz, C. Lienert, H. Komber, R. Friend and M. Sommer, *Polym. Chem.*, 2017, **8**, 4738–4745.
25 R. Matsidik, A. Luzio, S. Hameury, H. Komber, C. R. McNeill, M. Caironi and M. Sommer, *J. Mater. Chem. C*, 2016, **4**, 10371–10380.
26 R. M. Pankow, L. Ye, N. S. Gobalasingham, N. Salami, S. Samal and B. C. Thompson, *Polym. Chem.*, 2018, **9**, 3885–3892.
27 R. M. Pankow, L. Ye and B. C. Thompson, *Polym. Chem.*, 2018, **9**, 4120–4124.
28 R. M. Pankow, L. Ye and B. C. Thompson, *ACS Macro Lett.*, 2018, **7**, 1232–1236.
29 C. Capello, U. Fischer and K. Hungerbuhler, *Green Chem.*, 2007, **9**, 927–934.
30 T. Erdmenger, C. Guerrero-Sanchez, J. Vitz, R. Hoogenboom and U. S. Schubert, *Chem. Soc. Rev.*, 2010, **39**, 3317–3333.
31 P. G. Jessop, *Green Chemistry*, 2011, **13**, 1391.
32 P. Gandeepan, N. Kaplaneris, S. Santoro, L. Vaccaro and L. Ackermann, *ACS Sustainable Chem. Eng.*, 206, **4**, 6160-6166.
33 N. V. Tzouras, I. K. Stamatopoulos, A. T. Papastavrou, A. A. Liori and G. C. Vougioukalakis, *Coord. Chem. Rev.*, 2017, **343**, 25–138.
34 D. J. Burke and D. J. Lipomi, *Energy Environ. Sci.*, 2013, **6**, 2053–2066.
35 F. Chen, N. Li, X. Yang, L. Li, G. Li, S. Li, W. Wang, Y. Hu, A. Wang, Y. Cong, X. Wang and T. Zhang, *ACS Sustainable Chem. Eng.*, 2016, **4**, 6160–6166.
36 K. Watanabe, N. Yamagiwa and Y. Torisawa, *Org. Process Res. Dev.*, 2007, **11**, 251–258.

37 M. Renavd, P. D. Chantal and S. Kaliaguine, *The Canadian Journal of Chemical Engineering*, 1986, **64**, 787–791.
38 K. Jacobson, K. C. Maheria and A. Kumar Dalai, *Renewable and Sustainable Energy Reviews*, 2013, **23**, 91–106.
39 X. Wang and M. Wang, *Polym. Chem.*, 2014, **5**, 5784–5792.
40 D. Liu, B. Yang, B. Jang, B. Xu, S. Zhang, C. He, H. Y. Woo and J. Hou, *Energy Environ. Sci.*, 2017, **10**, 546–551.
41 P.-O. Morin, T. Bura, B. Sun, S. I. Gorelsky, Y. Li and M. Leclerc, *ACS Macro Lett.*, 2015, **4**, 21–24.
42 D. Leow, G. Li, T.-S. Mei and J.-Q. Yu, *Nature*, 2012, **486**, 518.
43 G. Li, L. Wan, G. Zhang, D. Leow, J. Spangler and J.-Q. Yu, *J. Am. Chem. Soc.*, 2015, **137**, 4391–4397.
44 O. K. Rasheed and B. Sun, *ChemistrySelect*, 2018, **3**, 5689–5708.
45 W. Lu, J. Kuwabara and T. Kanbara, *Macromol. Rapid Commun.*, 2013, **34**, 1151–1156.
46 J. Choi, K.-H. Kim, H. Yu, C. Lee, H. Kang, I. Song, Y. Kim, J. H. Oh and B. J. Kim, *Chem. Mater.*, 2015, **27**, 5230–5237.
47 R. Heuvel, F. J. M. Colberts, M. M. Wienk and R. A. J. Janssen, *J. Mater. Chem. C*, 2018, **6**, 3731–3742.
48 R. M. Pankow, N. S. Gobalasingham, J. D. Munteanu and B. C. Thompson, *J. Polym. Sci. Part A: Polym. Chem.*, 2017, **55**, 3370–3380.
49 R. M. Pankow, J. D. Munteanu and B. C. Thompson, *J. Mater. Chem. C*, 2018, **6**, 5992–5998.
50 N. S. Gobalasingham, R. M. Pankow and B. C. Thompson, *Polym. Chem.*, 2017, **8**, 1963–1971.
51 F. Grenier, K. Goudreau and M. Leclerc, *J. Am. Chem. Soc.*, 2017, **139**, 2816–2824.
52 R. Chinchilla and C. Nájera, *Chem. Rev.*, 2007, **107**, 874–922.
53 S. Beaupré and M. Leclerc, *J. Mater. Chem. A*, 2013, **1**, 11097–11105.
54 C. Amatore and A. Jutand, *Acc. Chem. Res.*, 2000, **33**, 314–321.
55 N. C. Bruno, M. T. Tudge and S. L. Buchwald, *Chem. Sci.*, 2013, **4**, 916–920.
56 M. Cong, Y. Fan, J.-M. Raimundo, J. Tang and L. Peng, *Org. Lett.*, 2014, **16**, 4074–4077.
57 F. Livi, N. S. Gobalasingham, E. Bundgaard and B. C. Thompson, *J. Polym. Sci., Part A: Polym. Chem.*, 2015, **53**, 2598–2605.
58 M. Fujitsuka, O. Ito, T. Yamashiro, Y. Aso and T. Otsubo, *J. Phys. Chem. A*, 2000, **104**, 4876–4881.
59 S. Zhang, L. Ye, H. Zhang and J. Hou, *Materials Today*, 2016, **19**, 533–543.
60 F. Proutiere and F. Schoenebeck, *Angewandte Chemie International Edition*, 2011, **50**, 8192–8195.
61 J. Kuwabara, K. Yamazaki, T. Yamagata, W. Tsuchida and T. Kanbara, *Polym. Chem.*, 2015, **6**, 891–895.
62 K. Sakamoto, Y. Takashima, N. Hamada, H. Ichida, H. Yamaguchi, H. Yamamoto and A. Harada, *Org. Lett.*, 2011, **13**, 672–675.
63 D. Zhou, N. Y. Doumon, M. Abdu-Aguye, D. Bartesaghi, M. A. Loi, L. J. Anton Koster, R. C. Chiechi and J. C. Hummelen, *RSC Adv.*, 2017, **7**, 27762–27769.
64 N. S. Gobalasingham, S. Noh and B. C. Thompson, *Polym. Chem.*, 2016, **7**, 1623–1631.
65 S. Lightowler and M. Hird, *Chem. Mater.*, 2005, **17**, 5538–5549.
66 A. E. Rudenko and B. C. Thompson, *J. Polym. Sci. A Polym. Chem.*, 2015, **53**, 135–147.
67 A. E. Rudenko, A. A. Latif and B. C. Thompson, *Nanotechnology*, 2014, **25**, 014005.
68 F. Livi, N. S. Gobalasingham, B. C. Thompson and E. Bundgaard, *J. Polym. Sci., Part A*, 2016, **54**, 2907–2918.
69 A. E. Rudenko and B. C. Thompson, *Macromolecules*, 2015, **48**, 569–575.
70 T. Kanbara, J. Kuwabara and W. Lu, *IOP Conf. Ser.: Mater. Sci. Eng.*, 2012, **54**, 012012.
71 T. Bura, S. Beaupré, M.-A. Légaré, J. Quinn, E. Rochette, J. T. Blaskovits, F.-G. Fontaine, A. Pron, Y. Li and M. Leclerc, *Chem. Sci.*, 2017, **8**, 3913–3925.
72 T. Kumada, Y. Nohara, J. Kuwabara and T. Kanbara, *BCSJ*, 2015, **88**, 1530–1535.
73 T. Morita, T. Satoh and M. Miura, *Organic Letters*, 2015, **17**, 4384–4387.
74 K. Ueda, S. Yanagisawa, J. Yamaguchi and K. Itami, *Angew. Chem. Int. Ed.*, 2010, **49**, 8946–8949.
75 K. Funaki, T. Sato and S. Oi, *Org. Lett.*, 2012, **14**, 6186–6189.
76 J. Chen, L. Wang, J. Yang, K. Yang, M. A. Uddin, Y. Tang, X. Zhou, Q. Liao, J. Yu, B. Liu, H. Y. Woo and X. Guo, *Macromolecules*, 2019, **52**, 341–353.
77 F. Liu, D. Chen, C. Wang, K. Luo, W. Gu, A. L. Briseno, J. W. P. Hsu and T. P. Russell, *ACS Appl. Mater. Interfaces*, 2014, **6**, 19876–19887.
78 R. M. Pankow, J. D. Munteanu and B. C. Thompson, *J. Mater. Chem. C*, 2018, **6**, 5992–5998.

ARTICLE

Influence of an Ester Directing-Group on Defect Formation in the Synthesis of Conjugated Polymers via Direct Arylation Polymerization (DArP) using Sustainable Solvents

Received 00th January 20xx,
Accepted 00th January 20xx

DOI: 10.1039/x0xx00000x

Robert M. Pankow[a], Liwei Ye[a], and Barry C. Thompson*[a]

Direct arylation polymerization (DArP) is a synthetic methodology that allows for the preparation of conjugated polymers via C-H activation, facilitating a streamlined synthetic pathway for accessing monomers, while providing a reduction in the number of synthetic steps, hazardous waste, and toxic reagents. Improving the aspects of sustainability by changing the solvent or transition metal catalyst to a more sustainable alternative has recently garnered attention, and constitutes great importance for establishing DArP as an appealing alternative to commonly employed polymerization methods. Interestingly, while directing-groups are often employed for various small-molecule C-H couplings, use of these moeities have remained relatively unexplored despite their potential to enhance the reactivity of a given monomer. Towards these ends, we explore the use of the sustainable solvents cyclopentyl methyl ether (CPME) and anisole for the synthesis of a diester functionalized bithiophene using DArP to afford the copolymer poly[5,5′-bis(2-butyloctyl)-(2,2′-bithiophene)-4,4′-dicarboxylate-alt-5,5′-2,2′-bithiophene] (PDCBT) with a molecular weight (Mn) of 13.8 kDa and a yield of 59%. However, we observe the likely presence of branching (β) defects through analysis of ^{1}H-NMR spectroscopy, GIXRD, and UV-vis absorption spectroscopy measurements. In order to determine if defect formation can be avoided, we study the occurance of defect formation as a function of the aryl spacer by employing the electron rich thieno[3,2-b]thiophene (PDCTT) and electron deficient 2,2′-bithiazole (PDCBTz). We find the optimal conditions provide PDCTT and PDCBTz with molecular weights of 26.4 and 4.9 kDa and yields of 90% and 46%, respectively, where PDCBTz was prone to form insoluble, branched polymer. This demonstrates that PDCBTz has a heightened reactivity towards defect formation, relative to PDCBT, while PDCTT does not, and indicates that such defect formation can be controlled through the appropriate selection of monomers. This study provides valuable insight regarding functional group tolerance and the capacity for esters to potentially function as directing-groups, leading to the undesired couplings of distal protons.

Introduction

Interest in conjugated polymers is ever increasing, due to the wide-range of potential applications these materials can be used for.[1,2] Primarily, their inclusion in organic electronic applications, such as light-emitting diodes, thin-film transistors, and photovoltaics is of considerable interest since they offer a low-cost alternative to their inorganic counterparts.[3–5] In particular, bulk-heterojunction polymer solar cells have experienced a renaissance of sorts due to the optimization of non-fullerene acceptors (NFA).[6–8] Power conversion efficiencies (PCE) in excess of 15% have been achieved in these devices, providing strong motivation to further advance this technology as a viable alternative energy source.[9,10] A polymer of interest in such solar cells is poly[5,5′-bis(2-butyloctyl)-(2,2′-bithiophene)-4,4′-dicarboxylate-alt-5,5′-2,2′-bithiophene] (PDCBT), which is shown in Scheme 1. This polymer has great potential, given its relative ease of synthesis (Scheme 2 and 3) and the performance in both

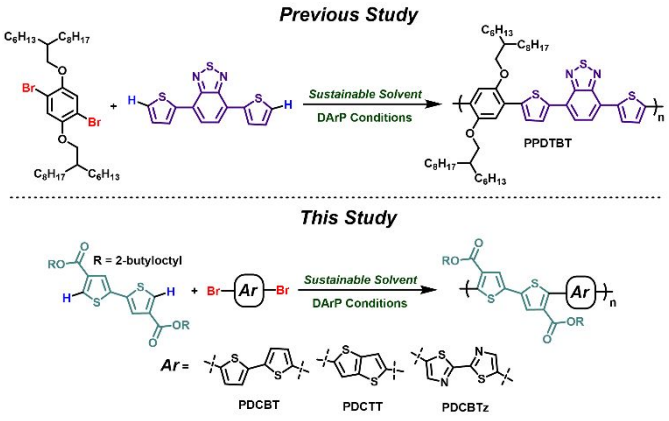

Scheme 1. Investigation of DArP using sustainable solvents towards the synthesis of PPDTBT (top), and the application of such solvents towards the synthesis of PDCBT, PDCBTT, and PDCBTz (bottom).

[a] Department of Chemistry and Loker Hydrocarbon Research Institute, University of Southern California, Los Angeles, California 90089-1661. Email: barrycth@usc.edu

Electronic Supplementary Information (ESI) available: [Monomer synthesis and characterization, Polymer characterization]. See DOI: 10.1039/x0xx00000x

fullerene (PCE of >7%) and non-fullerene (PCE of >10%) solar cells is very desirable.[11–15]The short synthetic procedure for PDCBT, based on only a few steps from commercial starting materials, is consistent with scalability, a key guiding principle of sustainability in conjugated polymers.[16,17] Another guiding principle is the avoidance of highly hazardous reagents, e.g. pyrophoric or acute toxicants, However, the synthesis of PDCBT, and almost all conjugated polymers used in solar cells are still reliant on Migita-Stille (Stille) polymerizations, which invoke the use of an alkylstannane moiety for transmetallation, or Suzuki-Miyaura (Suzuki) polymerizations, which require the inclusion of an organoboronate on the monomer. This undermines the sustainability of conjugated polymers, through the use of highly hazardous reagents, cryogenic conditions, and a large accumulation of toxic byproducts.

In contrast, direct arylation polymerization (DArP) provides an avenue for conjugated polymer synthesis that is streamlined and sustainable, via the direct functionalization of C-H bonds during the polymerization.[18–24] Research efforts towards further improving the sustainability of DArP protocols has increased, with studies that investigate changing the solvent or transition metal catalyst to more sustainable alternatives.[25–28] This change to sustainable sources, be it the solvent or transition metal catalyst, present major challenges as the chemistry associated with the desired chemical transformation can be highly dependent on the solvent or catalyst employed.[29,30] To further develop and improve upon such changes, a paradigm shift has occurred within organic chemistry to develop more sustainable reaction conditions.[31–33] Extension of this field to conjugated polymer synthesis, or polymer synthesis in general, is not a straightforward pursuit, as mentioned above.[30,34] This is why the focus on this area has expanded, since there are many challenges still to be faced with regards to finding broadly applicable, truly sustainable conditions for conjugated polymer synthesis. Recently, we have reported DArP conditions using cyclopentyl methyl ether (CPME), which is a sustainable solvent allowing for the synthesis of conjugated polymers with a minimized environmental impact.[26] CPME is advantageous for large scale applications because it can be prepared in a waste-free process with starting materials sourced from biomass, it is not classified as a reproductive toxin or carcinogen, and it is not a peroxide former like 2-methyltetrahydrofuran (2-MeTHF).[35,36]

From our previous study, the reaction conditions using CPME required extended times (72 hours) compared to comparable DArP protocols (16 hours). In regards to donor-acceptor copolymer synthesis, only a single copolymer, poly[(2,5-bis(2-hexyldecyloxy)phenylene)-alt-(4,7-di(thiophen-2-yl)benzo[c][1,2,5]thiadiazole) (PPDTBT), which is shown in Scheme 1 (top), was reported. Furthermore, the sustainable solvent anisole, which can be derived from biomass, does not form peroxides, and has been utilized for the fabrication of polymer solar cells with good efficiencies (PCE > 11%), was not studied.[37–40] With this in mind, we were emboldened to explore improved reaction conditions with sustainable solvents and apply them to a broader scope of monomers that have not been studied with DArP.

Herein, we report the synthesis of PDCBT using the sustainable solvents CPME and anisole, with a goal of elucidating the influence of monomer structure, specifically an ester directing group, on the capacity for defect formation, which is described below. We find that the most effective conditions with CPME allow for the rapid synthesis of PDCBT in less than 1 hour (M_n =13.6 kDa and yield of 59%, shown in Table 1), which is a significantly lower reaction time than the previously reported for PPDTBT (reaction time of 72 hours).[26] It was observed, however, that gelation of the polymerization can occur leading to insoluble material if the timing of the reaction is further extended. This is believed to be potentially due to the formation of crosslinking or branching (β) defects, which has been observed for bithiophene based copolymers prepared via DArP.[41] Through analysis using GIXRD, UV-vis absorption spectroscopy, and ^{1}H-NMR spectroscopy we show that branching (β) defects are the likely cause of this gelation. We propose that activation of β-protons on the bithiophene comonomer and subsequent defect formation is likely enhanced by the coordinative and directing ability of the ester moiety on the acceptor unit of PDCBT.[42–44] While many studies have been conducted to determine the formation of defects with DArP, the effect of a directing-group, such as an ester, has not been accounted for or previously realized.[45]

In order to explore the impact of the ester directing groups on the adjacent β-protons, we applied the polymerization conditions used for PDCBT towards the synthesis of poly[5,5′-bis(2-butyloctyl)-(2,2′-bithiophene)-4,4′-dicarboxylate -alt-2,5-[3,2-b]thienothiophene] (PDCTT) and poly[5,5′-bis(2-butyloctyl)-(2,2′-bithiophene)-4,4′-dicarboxylate -alt-5,5′-2,2′-bithiazole] (PDCBTz), which are shown in Scheme 1. The thieno[3,2-b]thiophene (TT) and 2,2′bithiazole (BTz) provide simple model compounds to study how a more electron rich monomer or electron deficient monomer may inhibit or accelerate the formation of branching defects, respectively. We find that branching occurs excessively with PDCBTz, preventing the isolation of high M_n polymer, but not PDCTT. This investigation and the findings herein provide valuable insight regarding functional group tolerance for DArP.

Experimental

General Methods.

All reagents were purchased from VWR and used as received, unless otherwise noted. $Pd(PPh_3)_2Cl_2$ was purchased from Beantown Chemical and used as received. Pd_2dba_3 was purchased from Matrix Scientific and used as received. P(*o*-anisyl)$_3$ was purchased from TCI and used as received. Cs_2CO_3 and K_2CO_3 were ground to a fine powder and dried in a vacuum oven (120 °C) overnight then stored in a desiccator before use. Anhydrous cyclopentyl methyl ether (CPME) was purchased from Acros Organics and used as received. Compounds **2-12** were prepared following literature procedures. See ESI for complete synthetic details in regards to monomer synthesis. 5,5′-bis(trimethylstannyl)-2,2′-bithiophene (13) used for Stille polymerization was previously prepared following literature procedure.[46]

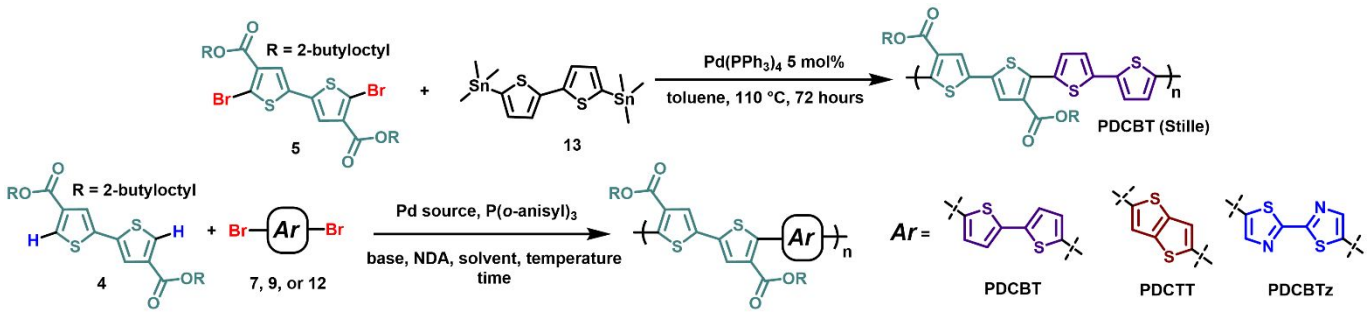

Scheme 2. Synthesis of PDCBT via Stille (top), and PDCBT, PDCTT, and PDCBTz via DArP (bottom).

Table 1 Detailed conditions and polymerization outcomes for the synthesis of PDCBT, PDCTT, and PDCBTz.

Entry	Polymer	Pd source[a]	Solvent (M)	Base (equiv.)	Temp. (°C)	Time (hours)	Yield (%)[b]	M_n (kDa)[b]	Đ[b]
1	PDCBT	Pd_2dba_3	THF (0.2)	Cs_2CO_3 (3)	120	16	NP	NP	NP
2	PDCBT	Pd_2dba_3	CPME (0.2)	Cs_2CO_3 (3.2)	110	16	72	7.9	2.08
3	PDCBT	$PdCl_2(PPh_3)_2$	CPME (0.2)	Cs_2CO_3 (3.2)	110	2	insoluble	insoluble	insoluble
4	PDCBT	$PdCl_2(PPh_3)_2$	CPME (0.2)	Cs_2CO_3 (3.2)	110	0.72	59	13.8	3.30
5[c]	PDCBT	$PdCl_2(PPh_3)_2$	CPME (0.2)	Cs_2CO_3 (2)	110	16	NP	NP	NP
6	PDCBT	$PdCl_2(PPh_3)_2$	CPME (0.2)	K_2CO_3 (3.2)	110	16	NP	NP	NP
7	PDCBT	$PdCl_2(PPh_3)_2$	Anisole (0.2)	Cs_2CO_3 (3.2)	110	16	77	8.3	2.13
8	PDCTT	$PdCl_2(PPh_3)_2$	CPME (0.2)	Cs_2CO_3 (3.2)	110	16	90	26.4	2.33
9	PDCBTz	$PdCl_2(PPh_3)_2$	CPME (0.2)	Cs_2CO_3 (3.2)	110	1.1	46	4.9	4.09
10	PDCBTz	$PdCl_2(PPh_3)_2$	CPME (0.2)	Cs_2CO_3 (3.2)	110	1	54	3.4	2.62
Stille	PDCBT	$Pd(PPh_3)_4$	Toluene (0.06)	-	110	72	95	24.0	3.08

[a]2 mol% loading for when Pd_2dba_3 is employed and 4 mol% for when $PdCl_2(PPh_3)_2$ is employed.[b] Determined after purification of the polymers via Soxhlet extraction. [c]Catalyst loading lowered from 4 mol% to 2 mol%. NP indicates an unsatisfactory or no precipitation from the reaction mixture prohibiting further purification.

All NMR were recorded at 25 °C using $CDCl_3$ on either a Varian Mercury 400 MHz, Varian VNMRS-500 MHz, or a Varian VNMR-600 MHz. All spectra were referenced to $CHCl_3$ (7.26 ppm), unless otherwise noted. Number average molecular weight (M_n) and polydispersity (Đ) were determined by size exclusion chromatography (SEC) using a Viscotek GPC Max VE 2001 separation module and a Viscotek Model 2501 UV detector, with 60 °C HPLC grade 1,2-dichlorobenzene (*o*-DCB) as eluent at a flow rate of 0.6 mL/min on one 300 × 7.8 mm TSK-Gel GMHHR-H column (Tosoh Corp). The instrument was calibrated vs. polystyrene standards (1050–3,800,000 g/mol), and data were analysed using OmniSec 4.6.0 software. Polymer samples were dissolved in HPLC grade o-dichlorobenzene at a concentration of 0.5 mg ml−1, stirred at 65 °C until dissolved, cooled to room temperature, and filtered through a 0.2 µm PTFE filter.

Scheme 3. Monomer synthesis.

For polymer thin-film measurements, solutions were spin-coated onto pre-cleaned glass slides from chloroform solutions at 7 mg/mL, which were then annealed at 150 °C for 30 minutes under N_2. UV–vis absorption spectra were obtained on a Perkin-Elmer Lambda 950 spectrophotometer. Thicknesses of the samples and grazing incidence X-ray diffraction (GIXRD) measurements were obtained using Rigaku diffractometer Ultima IV using a Cu Kα radiation source (λ = 1.54 Å) in the reflectivity and grazing incidence X-ray diffraction mode, respectively. Crystallite size was estimated using Scherrer's equation, shown with equation 1:

$$\tau = K\lambda/(\beta \cos\theta) \quad (1)$$

where τ is the mean size of the ordered domains, K is the dimensionless shape factor (K = 0.9), λ is the x-ray wavelength, β is the line broadening at half the maximum intensity (FWHM) in radians, and θ is the Bragg angle.

Synthesis of PDCBT via Stille.

To a 3-neck round bottom flask equipped with a stir-bar, nitrogen inlet, glass-stopper, Teflon septum, condenser, and under an inert, nitrogen atmosphere was added 5,5'-bis(trimethylstannyl)-2,2'-bithiophene (104 mg, 0.14 mmol, 1 equiv.) and **5** (68.5 mg, 0.14 mmol, 1 equiv.). Toluene (4.5 mL) was then added and the mixture degassed with N_2 for 20 minutes. $Pd(PPh_3)_4$ (11 mg, 0.007 mmol, 5 mol%) was added quickly to the flask, and it was then degassed again for 20 minutes. The Teflon septum was replaced with a glass stopper, and the mixture was then heated at 110 °C for 72 hours. $CHCl_3$ (5 mL) was added with gentle heating to dissolve the solids, and the mixture was precipitated into a chilled 10% NH_4OH/MeOH solution with high-stirring. The solids were then filtered into a Soxhlet thimble and purified via Soxhlet extraction (MeOH, hexanes, and $CHCl_3$). The $CHCl_3$ fraction was concentrated, transferred to a tared vial, the solvent stripped, and the polymer further dried overnight under vacuum (~100 mtorr).

^{1}H-NMR (500 MHz, $CDCl_3$): ^{1}H-NMR (500 MHz, $CDCl_3$): δ(ppm) 7.56-7.46 (br, 4H), 7.20 (br, 2H), 4.21 (d, *J* = 5.0 Hz, 4H), 1.75 (br, 2H), 1.32-1.28 (br, 32H), 0.91-0.86 (br, 12H). Consistent with literature reports.[47]

Synthesis of PDCBT via DArP (Entry 3 of Table 1)

An oven dried, high-pressure vessel (15 mL) was capped with an inverted red-rubber septum and cooled under a stream of nitrogen for 15 minutes. Compound 4 (100 mg, 0.17 mmol, 1 equiv.), neodecanoic acid (29 mg, 0.17 mmol, 1 equiv), 5,5'-dibromo-2,2'-bithiophene (55 mg, 0.17 mmol, 1 equiv.), P(*o*-anisyl)$_3$ (9.5 mg, 0.16 equiv), $PdCl_2(PPh_3)_2$ (4.77 mg, 0.0068 mmol, 0.04 equiv), and Cs_2CO_3 (180 mg, mmol, 3.2 equiv) was added. The vessel was then sparged with a stream of nitrogen for 10 minutes. CPME (1.7 mL), which was from a 5 mL stock that had been degassed prior with N_2 for 15 minutes, was quickly added and the rubber septum quickly replaced with a Teflon screwcap equipped with a rubber o-ring. The sealed vial was the placed into a preheated oil bath (110 °C) and stirred for 43 minutes. The vial was then removed from heat, $CHCl_3$ (5 mL) was added with gentle heating to dissolve the solids, and the mixture was precipitated into a chilled 10% NH_4OH/MeOH solution with high-stirring. The solids were then filtered into a Soxhlet thimble and purified via Soxhlet extraction (MeOH, hexanes, and $CHCl_3$). The $CHCl_3$ fraction was concentrated, transferred to a tared vial, the solvent stripped, and the polymer further dried overnight under vacuum (~100 mtorr). ^{1}H-NMR (500 MHz, $CDCl_3$): δ(ppm) 7.54-7.46 (br, 4H), 7.20 (br, 2H), 4.21 (d, *J* = 5.0 Hz, 4H), 1.75 (br, 2H), 1.32-1.28 (br, 32H), 0.91-0.86 (br, 12H). Consistent with literature reports.[47]

Synthesis of PDCTT via DArP (Entry 6 of Table 1).

Similar to that of PDCBT but with 5,5'-dibromo-2,2'-bithizaole (50.7 mg, 0.17 mmol, 1 equiv.) in place of 5,5'-dibromo-2,2'-bithiophene. ^{1}H-NMR (500 MHz, $CDCl_3$): δ(ppm) 7.76-7.57 (br, 4H), 4.19 (br, 4H), 1.76 (br, 2H), 1.29-0.79 (br, 44H). Consistent with literature reports.[47]

Synthesis of PDCBTz via DArP (Entry 7 of Table 1).

Similar to that of PDCBT but with 5,5'-dibromo-2,2'-bithizaole (55.4 mg, 0.17 mmol, 1 equiv.) in place of 5,5'-dibromo-2,2'-bithiophene. ^{1}H-NMR (600 MHz, $CDCl_3$): δ(ppm) 8.20-8.18 (br, 2H), 7.62-7.59 (br, 2H), 4.21 (br, 4H), 1.75 (br, 2H), 1.31-1.27 (br, 32H), 0.90-0.86 (br, 12H).

Results and Discussion

Polymer Synthesis of PDCBT via DArP

As depicted in **Scheme 3** (see ESI for complete details), the monomer syntheses follow similar routes to those found in the literature with the exception of compound **4**. It was found that the nickel-catalysed reductive homocoupling was low yielding (20-30%) in our hands, impeding the necessary scale-up to allow for the optimization of the polymerization step. Recently, Suzuki-Miyura conditions have been used for the preparation of similar compounds, albeit with simpler alkyl chains on the ester moiety, such as methyl or ethyl, and so these were successfully adapted to allow for a highly scalable synthesis of compound **4**. As reported by others, the bromination of compound **4**, which is required for Stille polymerization, proceeds with low levels of regio-selectivity leading to an inseparable byproduct if not performed carefully.[47] Due to these complications with the synthesis of monomer **5**, it was deemed that the donor should be halogenated for DArP studies considering that halogenation of the donor-units can proceed much more simply without harsh conditions, such as trifluoroacetic acid for a solvent. Furthermore, the high-pressure DArP conditions originally developed by Ozawa et al. and Leclerc et al., which we have demonstrated to be compatible with sustainable solvents, employ a halogenated donor-unit leaving the site for C-H activation on the acceptor-unit.[22,41] Thus, the functionalization pattern shown in Scheme 2, with the donor-unit being halogenated, was deemed the best route for polymer synthesis in general. Compounds **7**, **9**, and **12** were all prepared following their respective literature procedures.

As depicted in Scheme 2, with the results in Table 1 (Entry Stille), PDCBT was prepared via Stille polymerization following literature procedure with a M_n of 24 kDa in 95% yield.[11] An initial attempt for polymerization via DArP was performed using THF as a solvent, in order to see how polymerization proceeds using a more general and often applied set of conditions (Entry 1 of Table 1).[48,49] Interestingly, no polymer precipitate was formed after the reaction. This led us to conclude that the solvent, Pd-source, and temperature could be having an unforeseen, adverse effect on the synthesis of the polymer via DArP. Specifically, in regards to solvent, PDCBT prepared via Stille polymerization proceeds exclusively in toluene, directing us to believe that a more non-polar solvent may be beneficial. With this in mind, we chose CPME as the next solvent for study, given its development as a sustainable solvent for conjugated polymer synthesis and that it is less-polar than THF. As shown in Entry 2 of Table 1, changing the solvent from THF to CPME afforded polymer product in 72% yield with an M_n of 7.9 kDa.

As a next step, we chose to optimize the identity of the Pd-source, and we selected $PdCl_2(PPh_3)_2$ since it has been shown to provide an effective catalyst for DArP and other cross-coupling methodologies.[41,50–52] With the changes in solvent and Pd-source, we found that the polymerization mixture completely gelled in 2 hours, to yield a polymer product that was prohibitively insoluble (Entry 3 of Table 1). Specifically, the material isolated from the polymerization could not be isolated from the $CHCl_3$ or chlorobenzene (CB) Soxhlet fractions. This insolubility could be from achievement of a very high-M_n polymer product or from the introduction of defects due to undesired couplings, such as donor-donor homocouplings or branching (β) defects.[24,41,53] The cause of this observed catalyst dependence, can likely be traced to the higher reactivity for $PdCl_2(PPh3)_2$ in certain cross-coupling reactions and within DArP for certain monomers. Specifically, Leclerc et al. have reported conditions for the polymerization of substituted bithiophene based monomers using $PdCl_2(PPh_3)_2$ with P(o-anisyl)$_3$, achieving M_n of 52 kDa and a yield of 90%.[41] The results presented here as well as those described by Leclerc et al, indicate a preference for $PdCl_2(PPh_3)_2$ over Pd_2dba_3 when using bithiophene based monomers (Entries 2 and 4 of Table 1,

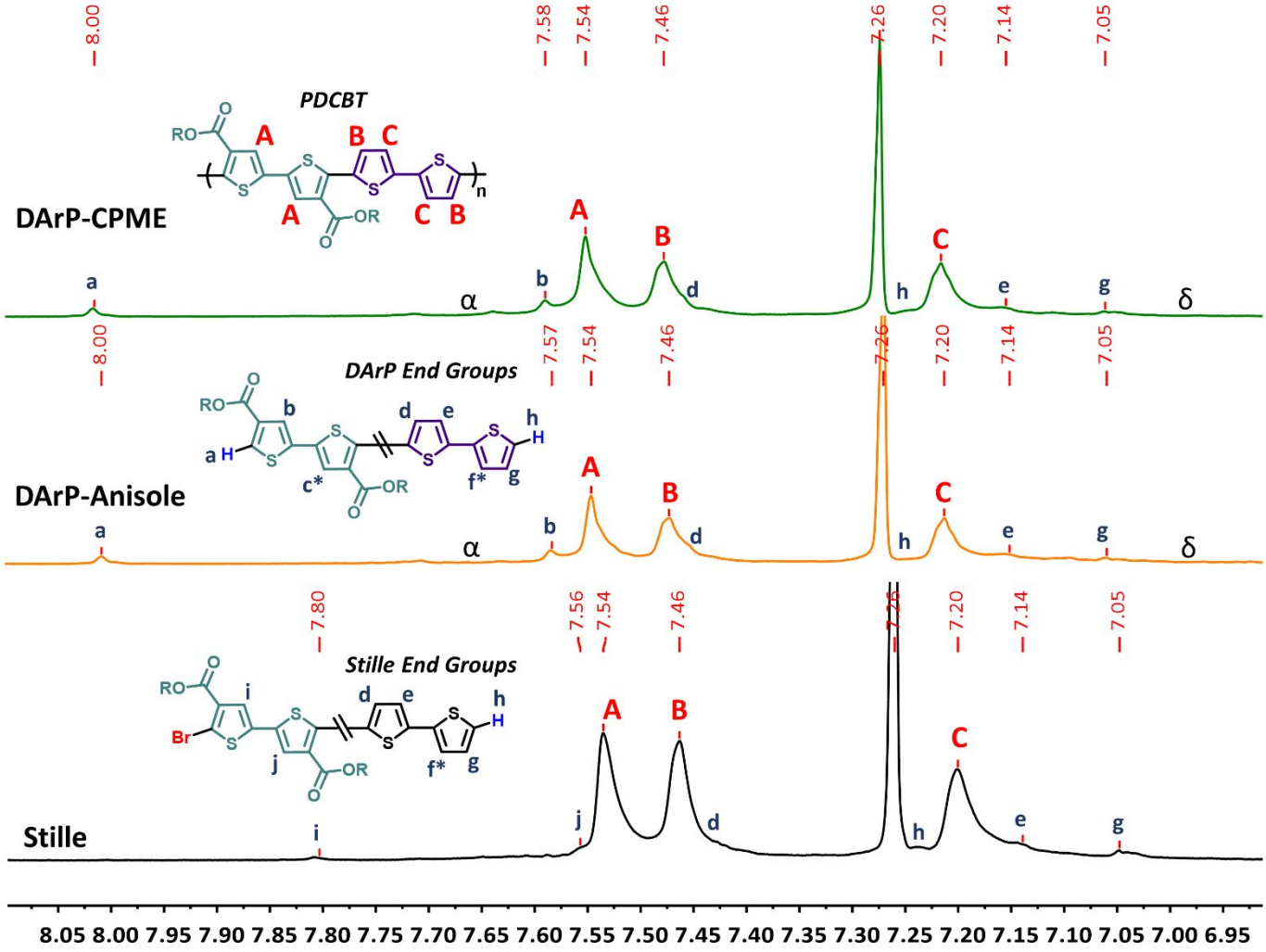

Figure 1. 1H-NMR ($CDCl_3$, 25 °C) of PDCBT prepared via DArP using the conditions outlined in Table 1: entry 4 (top), entry 7 (middle), and the Stille reference (bottom). End-group assignments are denoted by the lowercase letters (a-n) and the major resonances by the uppercase (A-C). For polymers prepared via DArP, acceptor-acceptor and donor-donor homocouplings are denoted by the characters, α and δ, respectively. Resonance labels with an asterisk (*) are not distinctly observed due to potential overlap (f* at 7.26 and c* at 7.55 ppm). All spectra referenced to $CHCl_3$ at 7.26 ppm.

respectively). Based on previous studies, $PdCl_2(PPh_3)_2$ has been shown to form anionic species ($Pd^0(L)_2(X)^{-1}$) from the highly reactive intermediate $Pd^0(L)_2$, both of which exhibit faster rates of oxidative addition than the $Pd^0(L)_4$ likely formed from Pd_2dba_3.[52,54] Formation of such a species, however, requires the in situ reduction of the Pd^{II}-precatalyst ($PdCl_2(PPh_3)_2$), which may only be a favorable process for only certain monomers, such as functionalized bithiophenes.[55] Furthermore, the dba ligand (from Pd_2dba_3) has been reported to stabilize the Pd^0 species to the point that it impedes catalysis or that it can interfere with the desired catalytic transformation, which may be occurring with the polymerizations described here.[55,56] While such reactivity is dependent on the monomers under study, such a heightened reactivity for $PdCl_2(PPh)_3$ is interesting given the prevalence of Pd_2dba_3 in donor-acceptor copolymer synthesis via DArP. To see if a soluble polymer product could be obtained that would allow for structural characterization, the reaction time was shortened and the polymerization was closely monitored so that it can be stopped just at the onset of gelation, where the polymerization changes from a red to violet-red color. It was found that after 43 minutes, or 0.72 hours, the onset of gelation occurs and a polymer product that exhibits good solubility (allowing for complete purification and isolation via Soxhlet extraction) is obtained (Entry 4 of Table 1) with a satisfactory M_n (13.8 kDa) and yield (59%). These conditions provide significant improvement from the original high-pressure THF based conditions originally used (no polymer product after 16 hours), and also the polymerizations reported in our previous study, where 72 hours was required to provide optimal results with CPME.[26] Additional efforts were made to control the observed high reactivity, by lowering the equivalents of Cs_2CO_3 from 3.2 to 2.0 and the catalyst loading from 4 mol% to 2 mol% (Entry 5 of Table 1) and changing the base to K_2CO_3 (Entry 6 of Table 1). However, these changes did not provide a satisfactory polymer precipitate from their respective reaction mixtures. With regards to changing the equivalents of base (Entry 5), the result of no polymer product forming is likely due to only 1 equivalent of reactive base (Cs_2CO_3) being present, with the remainder being quenched to $CsHCO_3$, as previously discussed by Ozawa et al.[22,57] Although

the catalyst loading has been lowered, going from 4 to 2 mol% will likely not have as detrimental of effect as lowering the base. This is because many DArP protocols, using similar conditions, use a catalyst loading of 1 to 2 mol%. In our previous study regarding sustainable solvents, we found that lowering the catalyst loading from 4 to 1 mol% actually led to an increase in Mn (from 31 to 41 kDa) for PPDTBT.[26] Furthermore, Leclerc's study regarding the DArP of dialkyl bithiophenes shows that the inherent reactivity of the monomer protons, such as the α or β protons, is what determines the propensity for defect formation for a given condition set, which is further discussed below.[41] Therefore, monomers with a greater potential for defect formation, such as those with an ester directing group, should be tailored or functionalized so as to prohibit the undesired activation of branching sites, since the tuning of reaction conditions, such as equivalents or identity of base and loading of catalyst, cannot necessarily allow for the exclusion of defects.

We were then interested to see the effect of changing the solvent, specifically with anisole. Anisole is less polar than THF with a dielectric constant of 4.33 versus 7.58 and, as described earlier, can be used as a more sustainable solvent for conjugated polymer synthesis and processing.[39,58,59] The dielectric constant is closer to that of CPME as well, which is at 4.76.[36] Interestingly, anisole was found to slow the rate of polymerization, by observation, since no gelation was observed (Entry 7 of Table 1). Consequentially, this led to a polymer with lower M_n (8.3 kDa), but an improved yield (77%). The dependence of the reaction on the choice of solvent is difficult to determine given the critical role of the solvent within this type of transformation, e.g. solubility of the base, coordination to palladium, and potential activation of halogens.[52,60,61] Given this, it is possible that the slight increase in polarity for CPME over anisole (4.76 versus 4.33, respectively) may help to stabilize transition states, intermediates, or provide improved solubility of the growing polymer chain. It is likely that through more extensive optimization or with a different copolymer the reaction time and outcome of the polymerization using anisole can be improved, and so anisole should not be discounted as a sustainable solvent for DArP.

^{1}H-NMR Characterization of DArP-PDCBT

To determine if the structure of the DArP-synthesized polymers match that of the known Stille synthesized PDCBT, ^{1}H-NMR spectroscopy was used, which is shown in Figure 1. The polymers, both those prepared using DArP and Stille, exhibited excellent solubility in chloroform allowing for well-defined resonances to be obtained in the spectra. As shown in Figure 1 (bottom spectrum), the Stille polymer shows three well defined resonances centered at 7.54, 7.46, and 7.20 ppm (A-C). These are in agreement with the observed literature values.[11,47] End-group assignments are based on the observed resonances for monomers and model compounds collected in $CDCl_3$ with identical or similar structure.[11,47,62] Interestingly, end-groups associated with destannylated bithiophene are observed at 7.25 ppm (label h, Figure 1). This is likely due to destannylation, which has been observed for electron-rich heterocyclic stannanes.[63]

For the polymers prepared via DArP (Figure 1, top and middle), the major resonances (A, B, and C) align very well with the Stille-reference polymer. Also, the smaller, distinct resonances (a-h, Figure 1) can be assigned to the expected end-groups of either the ester functionalized bithiophene or bithiophene, indicating good structural fidelity for the DArP polymers. Importantly, acceptor-acceptor homocoupling peaks (α), which can occur via an oxidative coupling and has been reported for monomers of similar structure, e.g. ester-functionalized thiophenes, are not observed at 7.66 ppm (Figure 1, top and middle).[50,64] An expanded view of this region (7.75-7.60 ppm) in the ESI (Figure S13), shows that acceptor-acceptor homocouplings are not present and that the small resonances near this point are also in the Stille-PDCBT. These smaller resonances present in both DArP-PDCBT and Stille-PDCBT likely correspond to the penultimate protons near the terminus of the polymer. Also, donor-donor homocouplings (δ) are not observed at 6.98 ppm.[65] End-groups corresponding to the bithiophene end-group are easily apparent (d-h, Figure 1). As with the Stille-reference, resonances corresponding to f* are not observed, likely due to overlap with the major resonance from solvent ($CHCl_3$) at 7.26 ppm. Shoulders near 7.45 ppm corresponding to proton d, are better defined in the DArP PDCBT polymers, compared with the Stille-reference. These results indicate that the conditions employed for entry 4 and 7 of Table 1 provide polymer product with good structural fidelity with regards to an absence of α and δ homocouplings, as observed by ^{1}H-NMR. Of the two homocoupling defects, δ homocouplings would be the likely cause of insoluble material to form, since no solubilizing alkyl chains are present on the bithiophene donor. Given their absence, in the case of Entry 4, this indicates that gelation and formation of insoluble material is likely occurring through crosslinking or β-defect formation, although these structural features are challenging to observe via ^{1}H-NMR.[24,41,66,67]

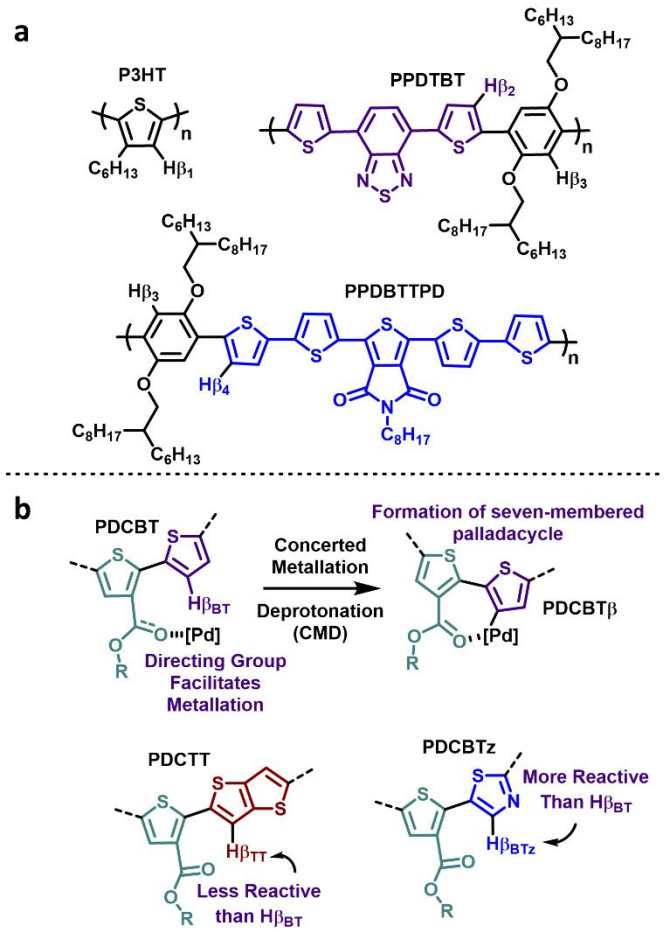

Figure 2. (a) Polymers (P3HT and PPDTBT) for which the DArP conditions were optimized allowing for the exclusion of defects (α, β, and δ), allowing for the application of these conditions to polymers with a greater potential for β-defect formation (PPDBTTPD). (b) Depiction of the directing group effect of the ester on PDCBT forming PDCBTβ, and the suppression or enhancement for β-defect formation when biaryls with different β-protons (PDCTT and PDCBTz) are used compared with PDCBT.

This conclusion on potential β-defect formation for PDCBT is reached based on previous DArP studies we have performed, which describe the defect free synthesis of P3HT and PPDTBT using similar conditions (Figure 2a).[26,68] Similar conditions were also applied towards the synthesis of PPDBTTPD (Figure 2a), which possesses numerous, unobstructed β-protons.[49] In each of these studies, no prohibitively insoluble material was obtained (even when precipitation during the polymerization was observed), and thorough characterization of these polymers confirmed an absence of β-defects. In the case of the aforementioned polymers (P3HT, PPDTBT, and PPDBTTPD), neodecanoic acid (NDA) inhibits β-defect formation by sterically shielding the β-protons ($H\beta_1$-$H\beta_4$) from the Pd-catalyst.[69] Since NDA is present (1 equiv.) in the DArP conditions reported here, β-defect formation must either be overcoming the steric hindrance or displacement of the NDA coordinated to Pd by the ester moiety is occurring. Esters, specifically, have been shown by Yu et al. to allow for the C-H activation of distal protons, via a seven-membered cyclopalladation, on electron rich arenes.[43] In the aforementioned study, the ester moiety displaced the carboxylic acid ligand used, allowing for C-H functionalization to occur. This type of reactivity is analogous to what we propose for PDCBT. Specifically, the ester directing group likely displaces the NDA and then the palladium metal center can form a seven-membered palladacycle with the adjacent thiophene aryl group (Figure 2b), which is based on the findings by Yu's aforementioned study. While directing groups (not carbonyl based) have been used in the synthesis of conjugated polymers via DArP, this mechanism of defect formation has not been explicitly observed to our knowledge.[70]

Synthesis of PDCTT and PDCBTz via DArP

As mentioned prior, the primary method for preventing β-defect formation in DArP is the use of a bulky carboxylic acid, such as NDA, but if carbonyl groups along the backbone can displace NDA then defect formation can occur. Applying the conditions then to a more reactive (BTz) and less reactive (TT) monomer would offer insight regarding how β-proton reactivity effects the propensity for defect formation (Figure 2b). Using these monomers for their respective copolymer synthesis, we expect to see an enhanced or uncontrollable level of defects with BTz and a suppression of such defects with TT relative to BT.

Describing BTz and TT as more and less reactive towards β-defect formation is based on previous studies in DArP and small-molecule C-H activation. Specifically, based on the previous studies by Leclerc et al. regarding the Gibbs free energy ($\Delta G^{\ddagger}_{298K}$) associated with C-H bond cleavage at the concerted metalation deprotonation (CMD) transition state (TS), the reactivity of β-protons for BTz ($\Delta G^{\ddagger}_{298K}$ = 26.7 kcal) should be

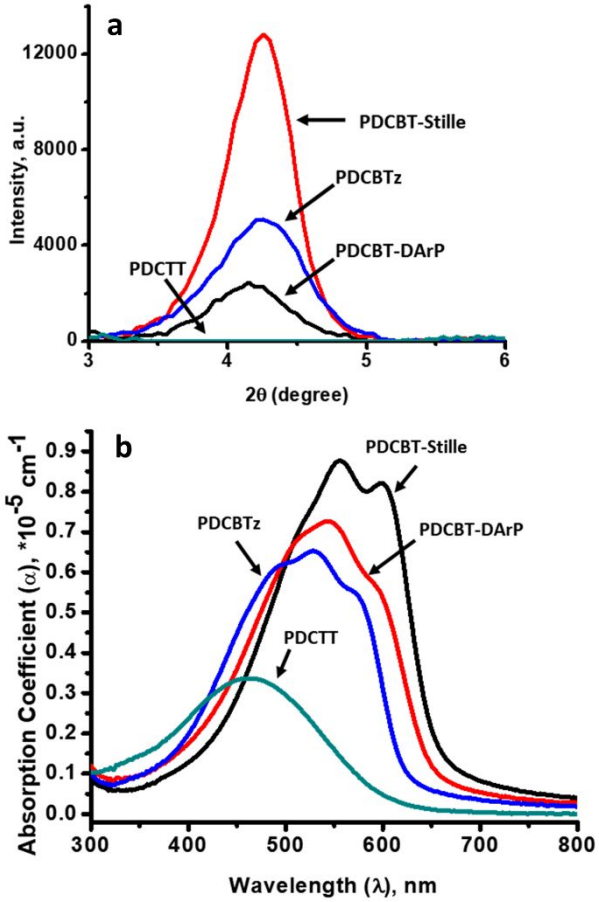

greater than that of BT ($\Delta G^{\ddagger}_{298K}$ = 28.3 kcal).[41,71] This type of calculation has not been performed for TT. However, low-reactivity for TT has been observed, where no polymerization proceeded via DArP unless a substituted TT was used to enhance its reactivity.[72] Furthermore, previous studies regarding the C-H activation of thieno[3,2-b]thiophene have concluded that Pd-catalysed oxidative conditions, which differ greatly from the ones employed here, are required for activation of the $H_{\beta TT}$ proton (Figure 2b), and that conditions reliant on the pKa of the proton, such as the ones employed for this study, do not provide coupled products in $H_{\beta TT}$ position.[73–75] In addition to a diminished reactivity, studies on the conformation of a TT unit flanked by carboxylate containing thiophenes, such as with PDCBT and PDCTT, have shown that twisting along the conjugated backbone occurs in the case of TT where BT is considered to be coplanar.[76] This twisting, which may be due to steric congestion brought upon by the more compact structure of the TT ring, leads to a large dihedral angle (>60°), which may inhibit formation of the seven-membered palladacycle intermediate (PDCBTβ, Figure 2b). Since BTz is structurally and spatially similar to BT, it is presumed that backbone twisting will not occur and that it should possess a nearly coplanar conformation as with PDCBT.

Confirming the ideas above, when the DArP conditions (Entry 4 of Table 1) that led to gelation with PDCBT were applied to PDCTT, we found that the polymerization mixture did not gel after 2 hours (Entry 8 of Table 1), and so the polymerization was left to go overnight (16 hours). After purification, it was found that the PDCTT obtained from this reaction provided a greater M_n (26 kDa) and yield (90%), relative to the same conditions for PDCBT. It should be noted that no $CHCl_3$-insoluble material was left-over after Soxhlet purification. It is likely that the extended reaction time contributes to the increase in yield and M_n, relative to PDCBT.[47] These results demonstrate that a monomer relatively with inert β-protons, compared to BT, can be employed when directing groups are present within the copolymer to successfully afford the desired copolymer.

When 2,2'-bithiazole was used, a reactivity for this monomer like that of bithiophene was observed. Specifically, onset of gelation of the reaction mixture was observed after 70 minutes leading to oligomeric material (M_n of 4.9 kDa with a yield of 46%) that could be isolated in the $CHCl_3$ fraction of the Soxhlet (Entry 9 of Table 1), but with a small portion that was prohibitively insoluble in the chloroform fraction of the Soxhlet. In order to see if a more soluble polymer product could be isolated with a decreased reaction time, as was observed with PDCBT, the polymerization was repeated but was stopped at 60 minutes (Entry 10 of Table 1). This afforded an oligomeric product that was entirely soluble in the $CHCl_3$ fraction of the Soxhlet (M_n of 3.4 kDa and 54% yield) with an improved yield albeit lower molecular weight. Based on these results, it is clear that the reaction conditions, which affords isolable polymer products for PDCBT and PDCTT with good molecular weights and yields, are not optimal or controllable for a more electron deficient monomer prone to activation of the β-proton, such as bithiazole. C-H activation of this proton ($H\beta_{BTz}$, Figure 2b) is presumed to be highly favourable, and as the concentration of the monomers decreases in the reaction mixture defect formation, such as crosslinking and branching, will likely become more favourable. This would make cross-linking or β-couplings highly competitive relative to the desired coupling for PDCBTz, leading to insoluble materials before polymer products of desirable molecular weights and yields can be obtained, as with PDCTT.

Although somewhat intuitive, this correlation between structure and reactivity provides a general guide for in applying this methodology towards the synthesis of other copolymers. Specifically, electron deficient monomers used in concert with directing groups may invoke undesired couplings when protons that can undergo C-H activation are within a reasonable proximity. Based on these results, it is presumed that this type of directing group effect is possible with PDCBT, causing the activation of undesired protons and leading to the observed gelation during the polymerization. The NMR spectra for all of the synthesized polymers is provided in the ESI and referenced to polymers of known structure, but ^{1}H-NMR is not a general method for determining the presence of β-defects. Therefore, we confirm their presence using GIXRD and UV-vis absorption spectroscopy.

GIXRD and UV-vis Characterization of Polymer Films

The inclusion of β-defects within a conjugated polymer backbone has pronounced effects on the thin-film structural and electronic properties. As a consequence of the disorder caused by the β-defect, coherent, periodic structure can be disrupted since ideal alignment of the polymer chains is

inhibited by the inclusion of a defect. This can be observed, as mentioned previously, using GIXRD and UV-vis absorption spectroscopy. With P3HT (Figure 2a) prepared via DArP as an example, β-defect content as little as 0.16% can shift d_{100}-spacing by 0.5 Å and noticeably decrease the intensity of the vibronic shoulder and the magnitude of the absorption coefficient in the UV-vis absorption spectrum in comparison to Stille-P3HT.[67] A similar trend is expected for the polymer PDCBT prepared via DArP, which is expected to contain β-defects.

As depicted in Figure 3 and shown in Table 2, the semi crystallinity and photophysical properties of the polymer thin-films vary, which can be attributed to differences in the polymer structure, molecular weights (M_n), and inclusion of β-defects. Specifically, the PDCBT prepared via Stille (Entry 1 of Table 2), which has a M_n of 26 kDa (Table 1) possess a peak absorption (λ_{max}) at 556 nm and an absorption coefficient (α) of 88 × 10^3 cm^{-1} (Figure 3b), while that prepared via the optimal DArP conditions (Entry 4 of Table 1), which has a M_n approximately half that of the Stille polymer at 13.8 kDa displays a blue shifted λ_{max} at 543 nm and an α of 73 × 10^3 cm^{-1} (Entry 2 of Table 2). In regards to semicrystallinity (Table 2 and Figure 3a), the difference between the DArP and Stille PDCBT polymers is clear, with a lower degree of crystallinity and crystallite size (13.4 versus 15.0 nm, respectively) for the PDCBT prepared via DArP.

Table 1. GIXRD and UV-vis absorbance data for PDCBT, PDCTT, and PDCBTz. [a]Measured on polymer films prepared from a 7 mg/mL chloroform solution and annealed at 150 °C for 30 minutes

Entry (Polymer)	Conditions Used (Table 1)	λ_{max} (nm)[a]; α (cm^{-1})[a]	d_{100} (Å)[a]	Crystallite Size (nm)[a]
1 (PDCBT)	Stille	556; 88 × 10^3	20.8	15.0
2 (PDCBT)	Entry 4	543; 73 × 10^3	21.3	13.4
3 (PDCTT)	Entry 8	463; 34 × 10^3	-	-
4 (PDCBTz)	Entry 9	529; 65 × 10^3	20.8	11.5

Figure 3. (a) GIXRD diffraction patterns for the polymers PDCBT-Stille, PDCBT-DArP, PDCTT, and PDCBTz. (b) Absorption profiles for the polymers PDCBT-Stille, PDCBT-DArP, PDCTT, and PDCBTz.

The d_{100}-spacing (21.3 and 20.8 Å, respectively) for these polymers is also different by 0.5 Å (Table 2 Entries 1 and 2). Taken as whole, the diminished intensity of the vibronic shoulder, the reduced absorption coefficient, and the increase in d_{100}-spacing provide significant evidence for β-defect formation.[67] While differences in polymer M_n could have an effect on the aborption profile, the differences are more likely ascribed to β-defect formation, since the M_n is greater than 10 kDa for the DArP-PDCBT (where polythiophenes are known to show saturation of their optical properties).[77] This conclusion is also based on our past observations with DArP and Stille-P3HT, as well PPDTBT (Figure 2a).[67,68]

In comparison to PDCBT, PDCTT (Entry 3 of Table 2) presents a rather featureless absorption profile (Figure 3b) with a blue shifted λ_{max} at 463 nm, similar to what has been previously reported (λ_{max} at 476 nm).[47] A vibronic shoulder was not expected with PDCTT since previous reports for this polymer depict a featureless absorption profile for the polymer prepared via Stille.[47] As discussed above, the diminished value for α (34 × 10^3 cm^{-1}) indicates a more disordered structure for this polymer, where orbital overlap of the π-system along the polymer backbone and the π-π interactions between polymer chains may be hindered due to twisting caused by steric-hindrance between the alkyl chains on the accepter unit.[76]Also, no diffraction was observed in the GIXRD measurements for this polymer further. As shown with previous studies, this is likely because temperatures in excess of 150 °C will be needed to induce crystallization and aggregation.[47,78] However, optimization of the thin-film morphology is not a focus of this study. Given that gelation did not occur with PDCTT and no insoluble material was observed after Soxhlet with $CHCl_3$, it is believed that presence of β-defects is highly minimized, if not excluded, for this polymer.

PDCBTz (Entry 4 of Table 2) shows an absorption profile similar to that of PDCBT (Figure 3b), with the appearance of a weak vibronic-shoulder and a λ_{max} at 529 nm (Figure 3b). It is notable that despite the more-electron deficient bithiazole unit being employed for this polymer, the blue shift for the polymer is rather slight (14 nm) versus the 80 nm observed for PDCTT. This provides further indication of how the donor unit for this class of polymers influences the planarity and orbital overlap of the π-system along the polymer backbone and the π-π interactions between polymer chains. In regards to semicrystallinity, PDCBTz (Entry 4 of Table 2) has a lamellar spacing of 20.8 Å, which is identical to the Stille-PDCBT polymer. However, the reduction in crystallite size, coupled with the weak vibronic shoulder in the UV-vis spectrum (Figure 3b), indicates that the PDCBTz isolated via DArP contains β-defects as was observed for PDCBT. These results provides evidence for the hypothesis that branching or cross-linking can be controlled by employing an electron-rich monomer that is more resilient against crosslinking or β-defect formation, such as TT. As described above, β-defect formation is supported when all the factors are taken into account. Specifically, in the synthesis of PDCBT and PDCBTz via DArP (see Table 2 for conditions) both lead to insoluble material, which is a major indication of a polymer laced with defects. ^{1}H-NMR confirms that δ-homocouplings, which could lead to insoluble material, are not occurring. GIXRD shows a reduction in the degree of crystallinity and a shift in the d-spacing consistent with β-defect formation. The UV-vis absorption profiles also show a reduction in the vibronic shoulder and the absorption coefficient. All of these pieces of evidence point to the likelihood of β-defect formation for the polymers PDCBT and PDCBTz, which leads to the formation of insoluble material during the polymerization.

Conclusions

In this study we presented the application of the sustainable solvents CPME and anisole towards the synthesis of PDCBT and its analogues, PDCTT and PDCBTz, via DArP. We find the diester moieties on the acceptor unit can function as directing groups enhancing the reactivity of the monomer designated for C-H bond functionalization providing a significant reduction in the

polymerization time. This enhancement in reactivity comes at the cost of selectivity, however, since crosslinking or β-defect formation occurs leading to the formation of insoluble polymer products. This likely occurs through displacement of the NDA, which is used to suppress β-defect formation, from the palladium catalyst by the ester. Through careful optimization, we were able to develop DArP conditions that allowed for the synthesis of isolable PDCBT in less than one hour, when CPME is used as the solvent, with a molecular weight (M_n) of 13.8 kDa and a yield of 59%. Application of the optimal conditions towards the relatively electron rich, PDCTT, which contains thieno[3,2-b]thiophene, and electron deficient, PDCBTz, which contains 2,2'-bithiazole, was performed to investigate the occurrence of defect formation by varying the aryl group. Specifically, electron deficient monomers may invoke cross-linking or branching defects due to the higher reactivity of the protons in the conjugated backbone of the polymer, which was observed with PDCBTz. However, with the electron-rich PDCTT a polymer product with a M_n of 26 kDa and a yield of 90% was obtained. Characterization using GIXRD and UV-vis absorption spectroscopy confirmed the presence of β-defects in PDCBT and PDCBTz prepared via DArP. This demonstrates an important need for understanding functional group tolerance and a guiding principle when developing conditions for DArP. Based on our results, a directing group can facilitate C-H activation of distal protons on adjacent aryl groups forming undesired defects, despite use of a bulky carboxylic acid ligand (NDA). Suppression of such defects is possible through the judicious selection of a comonomer, which contains a β-proton of low reactivity or can inhibit the formation of the intermediate metallocycle. Future work will focus on determining conditions that allow for the defect-free synthesis of electron deficient of conjugated copolymers, such as PDCBTz, using sustainable solvents, and determine conditions that allow for a more controlled synthesis when directing groups are employed.

Conflicts of interest

There are no conflicts to declare.

Acknowledgements

This work was supported by the National Science Foundation (MSN under award number CHE-1608891) and the Dornsife/Graduate School Fellowship (to R.M.P).

References

‡ 1 Oksana. Ostroverkhova, *Chem. Rev. (Washington, DC, U. S.)*, 2016, **116**, 13279–13412.
2 S. Inal, J. Rivnay, A.-O. Suiu, G. G. Malliaras and I. McCulloch, *Acc. Chem. Res.*, 2018, **51**, 1368–1376.
3 A. N. Sokolov, B. C.-K. Tee, C. J. Bettinger, J. B.-H. Tok and Zhenan. Bao, *Acc. Chem. Res.*, 2012, **45**, 361–371.
4 A. C. Grimsdale, K. Leok Chan, R. E. Martin, P. G. Jokisz and A. B. Holmes, *Chem. Rev.*, 2009, **109**, 897–1091.
5 B. C. Thompson and J. M. J. Frechet, *Angew. Chem., Int. Ed.*, 2008, **47**, 58–77.
6 Y. Lin, J. Wang, Z.-G. Zhang, H. Bai, Y. Li, D. Zhu and X. Zhan, *Adv. Mater.*, 2015, **27**, 1170–1174.
7 A. Wadsworth, M. Moser, A. Marks, M. S. Little, N. Gasparini, C. J. Brabec, D. Baran and I. McCulloch, *Chem. Soc. Rev.*, 2019, **48**, 1596–1625.
8 Y. Cai, L. Huo and Y. Sun, *Advanced Materials*, 2017, **29**, 1605437.
9 J. Yuan, Y. Zhang, L. Zhou, G. Zhang, H.-L. Yip, T.-K. Lau, X. Lu, C. Zhu, H. Peng, P. A. Johnson, M. Leclerc, Y. Cao, J. Ulanski, Y. Li and Y. Zou, *Joule*, 2019, **3**, 1140-1151.
10 H. Yao, Y. Cui, D. Qian, C. S. Ponseca, A. Honarfar, Y. Xu, J. Xin, Z. Chen, L. Hong, B. Gao, R. Yu, Y. Zu, W. Ma, P. Chabera, T. Pullerits, A. Yartsev, F. Gao and J. Hou, *J. Am. Chem. Soc.*, 2019, **141**, 7743-7750.
11 M. Zhang, X. Guo, W. Ma, H. Ade and J. Hou, *Adv. Mater.*, 2014, **26**, 5880–5885.
12 M. Chang, Y. Wang, Y.-Q.-Q. Yi, X. Ke, X. Wan, C. Li and Y. Chen, *J. Mater. Chem. A*, 2018, **6**, 8586–8594.
13 H. Feng, Y.-Q.-Q. Yi, X. Ke, Y. Zhang, X. Wan, C. Li and Y. Chen, *Solar RRL*, 2018, **2**, 1800053.
14 Y. Liu, L. Zuo, X. Shi, A. K.-Y. Jen and D. S. Ginger, *ACS Energy Lett.*, 2018, **3**, 2396-2403.
15 Y. Qin, M. A. Uddin, Y. Chen, B. Jang, K. Zhao, Z. Zheng, R. Yu, T. J. Shin, H. Y. Woo and J. Hou, *Advanced Materials*, 2016, **28**, 9416–9422.
16 J. E. Carlé, M. Helgesen, O. Hagemann, M. Hösel, I. M. Heckler, E. Bundgaard, S. A. Gevorgyan, R. R. Søndergaard, M. Jørgensen, R. García-Valverde, S. Chaouki-Almagro, J. A. Villarejo and F. C. Krebs, *Joule*, 2017, **1**, 274–289.
17 N. S. Gobalasingham, J. E. Carle, F. C. Krebs, B. C. Thompson, E. Bundgaard and Martin. Helgesen, *Macromol. Rapid Commun.*, 2017, **38**, 1700526.
18 P.-O. Morin, T. Bura and M. Leclerc, *Mater. Horiz.*, 2015, **3**, 11–20.
19 N. S. Gobalasingham and B. C. Thompson, *Progress in Polymer Science*, 2018, **83**, 135–201.
20 H. Bohra and M. Wang, *Journal of Materials Chemistry A*, 2017, **5**, 11550–11571.
21 K. Okamoto, J. Zhang, J. B. Housekeeper, S. R. Marder and C. K. Luscombe, *Macromolecules*, 2013, **46**, 8059–8078.

22 M. Wakioka, Y. Kitano and F. Ozawa, *Macromolecules*, 2013, **46**, 370–374.
23 Y. Fujinami, J. Kuwabara, W. Lu, H. Hayashi and T. Kanbara, *ACS Macro Lett.*, 2012, **1**, 67–70.
24 F. Lombeck, F. Marx, K. Strassel, S. Kunz, C. Lienert, H. Komber, R. Friend and M. Sommer, *Polym. Chem.*, 2017, **8**, 4738–4745.
25 R. Matsidik, A. Luzio, S. Hameury, H. Komber, C. R. McNeill, M. Caironi and M. Sommer, *J. Mater. Chem. C*, 2016, **4**, 10371–10380.
26 R. M. Pankow, L. Ye, N. S. Gobalasingham, N. Salami, S. Samal and B. C. Thompson, *Polym. Chem.*, 2018, **9**, 3885–3892.
27 R. M. Pankow, L. Ye and B. C. Thompson, *Polym. Chem.*, 2018, **9**, 4120–4124.
28 R. M. Pankow, L. Ye and B. C. Thompson, *ACS Macro Lett.*, 2018, **7**, 1232–1236.
29 C. Capello, U. Fischer and K. Hungerbuhler, *Green Chem.*, 2007, **9**, 927–934.
30 T. Erdmenger, C. Guerrero-Sanchez, J. Vitz, R. Hoogenboom and U. S. Schubert, *Chem. Soc. Rev.*, 2010, **39**, 3317–3333.
31 P. G. Jessop, *Green Chemistry*, 2011, **13**, 1391.
32 P. Gandeepan, N. Kaplaneris, S. Santoro, L. Vaccaro and L. Ackermann, *ACS Sustainable Chem. Eng.*, 206, **4**, 6160-6166.
33 N. V. Tzouras, I. K. Stamatopoulos, A. T. Papastavrou, A. A. Liori and G. C. Vougioukalakis, *Coord. Chem. Rev.*, 2017, **343**, 25–138.
34 D. J. Burke and D. J. Lipomi, *Energy Environ. Sci.*, 2013, **6**, 2053–2066.
35 F. Chen, N. Li, X. Yang, L. Li, G. Li, S. Li, W. Wang, Y. Hu, A. Wang, Y. Cong, X. Wang and T. Zhang, *ACS Sustainable Chem. Eng.*, 2016, **4**, 6160–6166.
36 K. Watanabe, N. Yamagiwa and Y. Torisawa, *Org. Process Res. Dev.*, 2007, **11**, 251–258.
37 M. Renavd, P. D. Chantal and S. Kaliaguine, *The Canadian Journal of Chemical Engineering*, 1986, **64**, 787–791.
38 K. Jacobson, K. C. Maheria and A. Kumar Dalai, *Renewable and Sustainable Energy Reviews*, 2013, **23**, 91–106.
39 X. Wang and M. Wang, *Polym. Chem.*, 2014, **5**, 5784–5792.
40 D. Liu, B. Yang, B. Jang, B. Xu, S. Zhang, C. He, H. Y. Woo and J. Hou, *Energy Environ. Sci.*, 2017, **10**, 546–551.
41 P.-O. Morin, T. Bura, B. Sun, S. I. Gorelsky, Y. Li and M. Leclerc, *ACS Macro Lett.*, 2015, **4**, 21–24.
42 D. Leow, G. Li, T.-S. Mei and J.-Q. Yu, *Nature*, 2012, **486**, 518.
43 G. Li, L. Wan, G. Zhang, D. Leow, J. Spangler and J.-Q. Yu, *J. Am. Chem. Soc.*, 2015, **137**, 4391–4397.
44 O. K. Rasheed and B. Sun, *ChemistrySelect*, 2018, **3**, 5689–5708.
45 W. Lu, J. Kuwabara and T. Kanbara, *Macromol. Rapid Commun.*, 2013, **34**, 1151–1156.
46 J. Choi, K.-H. Kim, H. Yu, C. Lee, H. Kang, I. Song, Y. Kim, J. H. Oh and B. J. Kim, *Chem. Mater.*, 2015, **27**, 5230–5237.
47 R. Heuvel, F. J. M. Colberts, M. M. Wienk and R. A. J. Janssen, *J. Mater. Chem. C*, 2018, **6**, 3731–3742.
48 R. M. Pankow, N. S. Gobalasingham, J. D. Munteanu and B. C. Thompson, *J. Polym. Sci. Part A: Polym. Chem.*, 2017, **55**, 3370–3380.
49 R. M. Pankow, J. D. Munteanu and B. C. Thompson, *J. Mater. Chem. C*, 2018, **6**, 5992–5998.
50 N. S. Gobalasingham, R. M. Pankow and B. C. Thompson, *Polym. Chem.*, 2017, **8**, 1963–1971.
51 F. Grenier, K. Goudreau and M. Leclerc, *J. Am. Chem. Soc.*, 2017, **139**, 2816–2824.
52 R. Chinchilla and C. Nájera, *Chem. Rev.*, 2007, **107**, 874–922.
53 S. Beaupré and M. Leclerc, *J. Mater. Chem. A*, 2013, **1**, 11097–11105.
54 C. Amatore and A. Jutand, *Acc. Chem. Res.*, 2000, **33**, 314–321.
55 N. C. Bruno, M. T. Tudge and S. L. Buchwald, *Chem. Sci.*, 2013, **4**, 916–920.
56 M. Cong, Y. Fan, J.-M. Raimundo, J. Tang and L. Peng, *Org. Lett.*, 2014, **16**, 4074–4077.
57 F. Livi, N. S. Gobalasingham, E. Bundgaard and B. C. Thompson, *J. Polym. Sci., Part A: Polym. Chem.*, 2015, **53**, 2598–2605.
58 M. Fujitsuka, O. Ito, T. Yamashiro, Y. Aso and T. Otsubo, *J. Phys. Chem. A*, 2000, **104**, 4876–4881.
59 S. Zhang, L. Ye, H. Zhang and J. Hou, *Materials Today*, 2016, **19**, 533–543.
60 F. Proutiere and F. Schoenebeck, *Angewandte Chemie International Edition*, 2011, **50**, 8192–8195.
61 J. Kuwabara, K. Yamazaki, T. Yamagata, W. Tsuchida and T. Kanbara, *Polym. Chem.*, 2015, **6**, 891–895.
62 K. Sakamoto, Y. Takashima, N. Hamada, H. Ichida, H. Yamaguchi, H. Yamamoto and A. Harada, *Org. Lett.*, 2011, **13**, 672–675.
63 D. Zhou, N. Y. Doumon, M. Abdu-Aguye, D. Bartesaghi, M. A. Loi, L. J. Anton Koster, R. C. Chiechi and J. C. Hummelen, *RSC Adv.*, 2017, **7**, 27762–27769.
64 N. S. Gobalasingham, S. Noh and B. C. Thompson, *Polym. Chem.*, 2016, **7**, 1623–1631.

65 S. Lightowler and M. Hird, *Chem. Mater.*, 2005, **17**, 5538–5549.
66 A. E. Rudenko and B. C. Thompson, *J. Polym. Sci. A Polym. Chem.*, 2015, **53**, 135–147.
67 A. E. Rudenko, A. A. Latif and B. C. Thompson, *Nanotechnology*, 2014, **25**, 014005.
68 F. Livi, N. S. Gobalasingham, B. C. Thompson and E. Bundgaard, *J. Polym. Sci., Part A*, 2016, **54**, 2907–2918.
69 A. E. Rudenko and B. C. Thompson, *Macromolecules*, 2015, **48**, 569–575.
70 T. Kanbara, J. Kuwabara and W. Lu, *IOP Conf. Ser.: Mater. Sci. Eng.*, 2012, **54**, 012012.
71 T. Bura, S. Beaupré, M.-A. Légaré, J. Quinn, E. Rochette, J. T. Blaskovits, F.-G. Fontaine, A. Pron, Y. Li and M. Leclerc, *Chem. Sci.*, 2017, **8**, 3913–3925.
72 T. Kumada, Y. Nohara, J. Kuwabara and T. Kanbara, *BCSJ*, 2015, **88**, 1530–1535.
73 T. Morita, T. Satoh and M. Miura, *Organic Letters*, 2015, **17**, 4384–4387.
74 K. Ueda, S. Yanagisawa, J. Yamaguchi and K. Itami, *Angew. Chem. Int. Ed.*, 2010, **49**, 8946–8949.
75 K. Funaki, T. Sato and S. Oi, *Org. Lett.*, 2012, **14**, 6186–6189.
76 J. Chen, L. Wang, J. Yang, K. Yang, M. A. Uddin, Y. Tang, X. Zhou, Q. Liao, J. Yu, B. Liu, H. Y. Woo and X. Guo, *Macromolecules*, 2019, **52**, 341–353.
77 F. Liu, D. Chen, C. Wang, K. Luo, W. Gu, A. L. Briseno, J. W. P. Hsu and T. P. Russell, *ACS Appl. Mater. Interfaces*, 2014, **6**, 19876–19887.
78 R. M. Pankow, J. D. Munteanu and B. C. Thompson, *J. Mater. Chem. C*, 2018, **6**, 5992–5998.

Table of Contents Entry

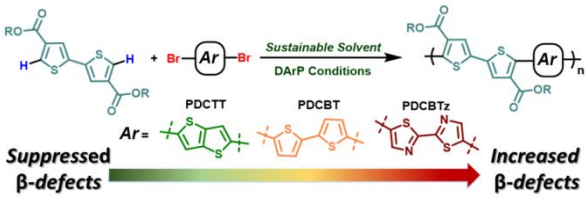

We report the application of green solvents in DArP and the structure-dependent β-defect formation due to an ester directing group.

Supporting Information

Influence of an Ester Directing-Group on Defect Formation in the Synthesis of Conjugated Polymers via Direct Arylation Polymerization (DArP) using Sustainable Solvents

Robert M. Pankow, Liwei Ye, and Barry C. Thompson*

Department of Chemistry and Loker Hydrocarbon Research Institute, University of Southern California, Los Angeles, California 90089-1661

*Email: barrycth@usc.edu

1. General

All reactions were performed under dry N_2 in oven dried glassware, unless otherwise noted. Unless otherwise noted, all reagents were purchased and used as received from commercial sources. Solvents were purchased from VWR and used without purification, unless otherwise noted. Anhydrous, unstabilized cyclopentyl methyl ether (CPME) was purchased and used as received. Cs_2CO_3 was ground into a fine powder and dried at 120 °C in a vacuum oven before use. 5,5'-bis(trimethylstannyl)-2,2'-bithiophene was previously prepared following literature procedure.[1] All NMR were recorded at 25 °C using $CDCl_3$ on either a Varian Mercury 400 MHz, Varian VNMRS-500 MHz, or a Varian VNMR-600 MHz. All spectra were referenced to $CHCl_3$ (7.26 ppm), unless otherwise noted. Number average molecular weight (M_n) and polydispersity (Đ) were determined by size exclusion chromatography (SEC) using a Viscotek GPC Max VE 2001 separation module and a Viscotek Model 2501 UV detector, with 60 °C HPLC grade 1,2-dichlorobenzene (*o*-DCB) as eluent at a flow rate of 0.6 mL/min on one 300 × 7.8 mm TSK-Gel GMHHR-H column (Tosoh Corp). The instrument was calibrated vs. polystyrene standards (1050−3,800,000 g/mol), and data were analysed using OmniSec 4.6.0 software. Polymer samples were dissolved in HPLC grade o-dichlorobenzene at a concentration of 0.5 mg ml^{-1}, stirred at 65 °C until dissolved, cooled to room temperature, and filtered through a 0.2 μm PTFE filter.

For polymer thin-film measurements, solutions were spin-coated onto pre-cleaned glass slides from *o*-dichlorobenzene (*o*-DCB) solutions at 7 mg/mL. UV−vis absorption spectra were obtained on a Perkin-Elmer Lambda 950 spectrophotometer. Thicknesses of the samples and grazing incidence X-ray diffraction (GIXRD) measurements were obtained using Rigaku diffractometer Ultima IV using a Cu Kα radiation source (λ = 1.54 Å) in the reflectivity and

grazing incidence X-ray diffraction mode, respectively. Crystallite size was estimated using Scherrer's equation:

$$\tau = K\lambda/(\beta \cos\theta) \qquad (1)$$

where τ is the mean size of the ordered domains, K is the dimensionless shape factor (K = 0.9), λ is the x-ray wavelength, β is the line broadening at half the maximum intensity (FWHM) in radians, and θ is the Bragg angle.

2. Monomer Synthesis

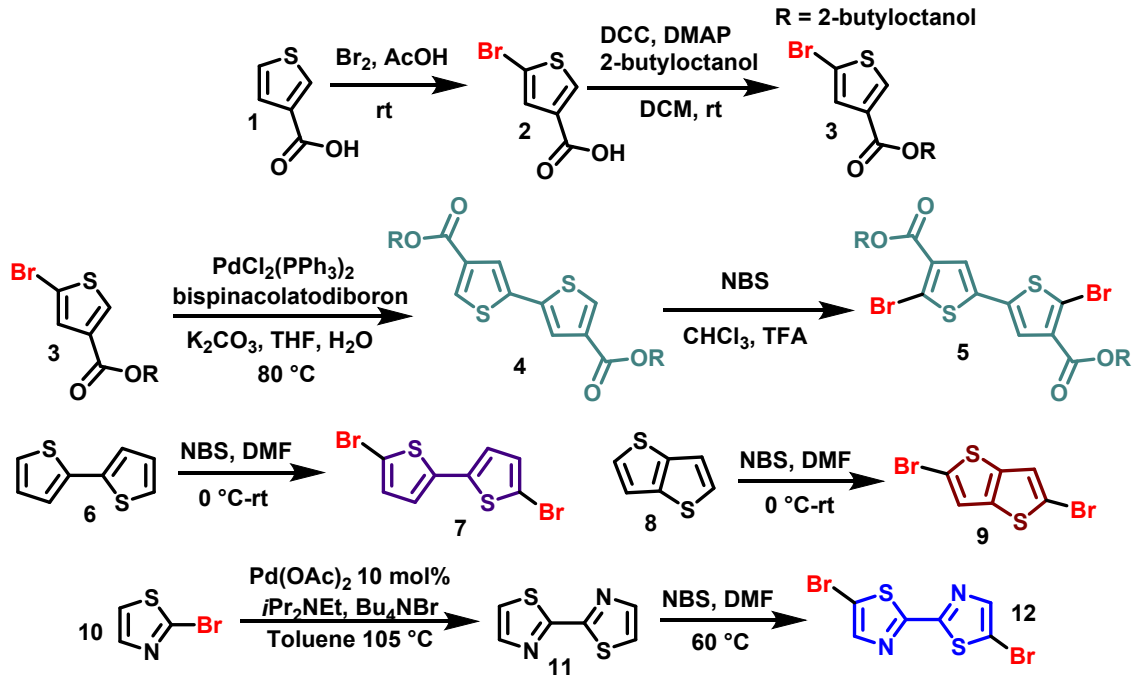

Scheme S1. Monomer Synthesis.

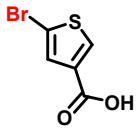

Synthesis of 5-bromothiophene-3-carboxylic acid (**2**):
To an Erlenmeyer flask equipped with a stir-bar, 3-thiophene carboxylic acid (10 g, 78 mmol, 1 equiv) was dissolved in glacial acetic acid (60 mL). To this, a solution of bromine (5.61 g, 35.1 mmol, 0.9 equiv) in glacial acetic acid (30 mL) was added slowly. The mixture was allowed to stir for 1 hour and then it was poured in water (300 mL) and stirred for 15 minutes. The solid was filtered off and washed with water. It was then recrystallized from water (300 mL), filtered,

and dried in under vacuum (~100 mtorr) overnight. 5.83 g, 41%. ^{1}H-NMR 400 MHz ($CDCl_3$): δ (ppm) 8.11 (d, *J* = 1.6 Hz, 1H), 7.51 (d, *J* = 1.6 Hz, 1H). Consistent with literature reports.[2]

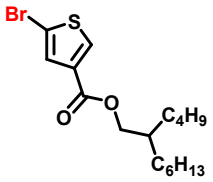

Synthesis of 2-butyloctyl-5-bromothiophene-3-carboxylate (**3**)
In an oven-dried 3-neck roundbottom flask equipped with a N_2 inlet and a stirbar **2** (4.00 g, 19.3 mmol, 1 equiv), DMAP (0.826 g, 23.16 mmol, 0.35 equiv), and DCC (4.78 g, 23.16 mmol, 1.2 equiv), were dissolved in anhydrous DCM (50 mL). This mixture was allowed to stir for 30 minutes. To this, 2-butyloctanol (5.39 g, 28.95 mmol, 1.5 equiv) was added dropwise via syringe. The mixture was then stirred for 48 hours. The precipitate was filtered off, it was diluted with water (50 mL), and it was extracted with DCM. The organic extracts were then washed with brine and dried with Na_2SO_4. The solvent was stripped and it was purified using column chromatography (15% DCM/hexanes). 6.30 g, 87%. ^{1}H-NMR 400 MHz ($CDCl_3$): δ (ppm) 7.97 (d, *J* = 1.6, 1H), 7.45 (d, *J* = 1.6 Hz, 1 H), 4.16 (d, *J* = 5.6 Hz, 2H), 1.74-1.69 (m, 1H), 1.35-1.28 (m, 16H), 0.91-0.86 (m, 6H). Consistent with literature reports.[3]

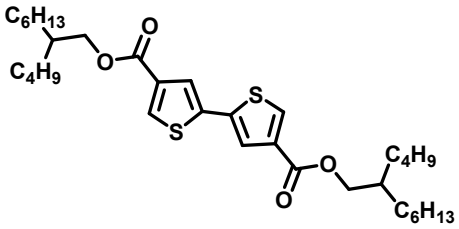

Synthesis of Bis(2-butyloctyl)[2,2'-bithiophene]-4,4'-dicarboxylate (**4**):
To a 3-neck round bottom flask equipped with a stir-bar, nitrogen inlet, glass-stopper, Teflon septum, and condenser was added potassium carbonate (9.1 g, 66 mmol, 4 equiv) and bispinacolatodiboron (2.09 g, 8.23 mmol, 0.5 equiv). The flask was evacuated and refilled with N_2 3 times. Compound 3 (6.18 g, 16.46 mmol, 1 equiv) and a 50 mL mixture of THF:H_2O (3:1) was then added, and the mixture was degassed for 20 minutes. $Pd(PPh_3)_2Cl_2$ (693 mg, 0.99 mmol, 0.06 equiv) was quickly added and the mixture degassed for an additional 20 minutes. The Teflon septum was replaced with a glass stopper, and the mixture was then heated at 80 °C for 24 hours. The reaction was cooled and extracted with DCM. The extracts were washed with brine, dried with Na_2SO_4, and chromatographed using a solvent gradient of 10% DCM/hexanes to 30% DCM/hexanes to afford a pale yellow, viscous oil (69% yield). ^{1}H-NMR 400 MHz ($CDCl_3$): δ (ppm) 7.98 (d, *J* = 1.2 Hz, 2H), 7.57 (d, *J* = 1.2 Hz, 2H), 4.19 (d, *J* = 6.0 Hz, 4H), 1.77-1.73 (m, 2H), 1.39-1.27 (m, 32H), 0.93-0.86 (m, 12H). Consistent with literature reports.[3]

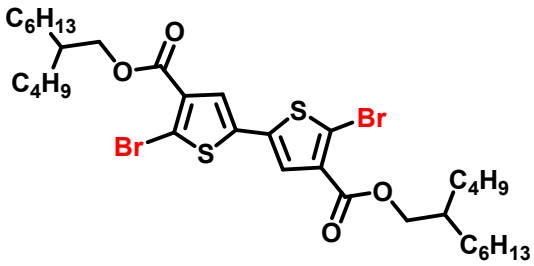

Synthesis of Bis(2-butyloctyl)[2,2'-bithiophene]-4,4'-dicarboxylate (**5**):
To a scintillation vial equipped with a screw cap and stir bar was added **4** (267 mg, 0.45 mmol, 1 equiv.), $CHCl_3$ (2 mL), and trifluoroactetic acid (0.5 mL). The vial was wrapped with foil to shield it from light, and NBS (160.2 mg, 0.9 mmol, 2 equiv.) was added portion wise and it was allowed to stir for 16 hours. In order to reach completion, an additional 16 mg, 0.2 equiv, of NBS and 1.5 mL of TFA were added and it was allowed to stir for an additional 4 hours. The reaction mixture was then diluted with water (10 mL) and extracted with $CHCl_3$. The organic extracts were then washed with brine and dried with Na_2SO_4. Purification was performed using column chromatography (20% DCM/hexanes). 197 mg, 59%. ^{1}H-NMR 500 MHz ($CDCl_3$): δ (ppm) 7.35 (s, 2H), 4.21 (d, J = 5.5 Hz, 4H), 1.75-1.73 (m, 2H), 1.41-1.27 (m, 32H), 0.91-0.86 (m, 12H). Consistent with literature reports.[2,3]

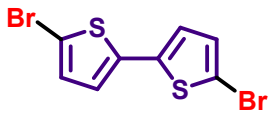

Synthesis of 5,5'-dibromo-2,2'-bithiophene (**7**):
To 3-neck roundbottom flask equipped with a N_2 inlet and a stirbar **6** (2.0 g, 12.0 mmol, 1 equiv) was added and dissolved in DMF (50 mL). The mixture was then cooled to 0 ˚C and NBS (4.28 g, 24.06 mmol, 2 equiv.) was added in one portion. This was allowed to slowly warm-up to room temperature with stirring overnight. The mixture was then poured into water (250 mL) and recrystallized from a mixtures of hexanes/$CHCl_3$. 2.84 g, 73%. ^{1}H-NMR 400 MHz ($CDCl_3$): δ (ppm) 6.96 (d, J = 4.0 Hz), 2H), 6.85 (d, J = 4.0 HZ, 2H). Consistent with literature reports.[4]

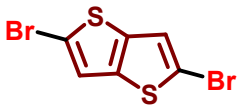

Synthesis of 2,5-dibromothieno[3,2-b]thienothiophene (**9**):
Thineno[3,2-b]thiophene (500 mg, 3.57 mmol, 1 equiv) was added to a 3-neck round bottom flask equipped with a stir-bar, which was then vacuum-backfilled with N_2 three times. DMF (7 mL) was added and the solution was degassed for 15 minutes. It was then cooled to 0 ˚C and NBS (1.27 g, 7.13 mmol, 2 equiv.) was added in one portion. The mixture was then stirred for 3 hours, allowing it to warm to room temperature. Water was added (15 mL) and a precipitate formed that was then filtered, washed with water, and dried under high-vacuum. The crude product was then recrystallized using a mixture of EtOH/$CHCl_3$. 460 mg, 43%.^{1}H-NMR 400 MHz ($CDCl_3$): δ (ppm) 7.17 (s, 2H). Consistent with literature reports.[5]

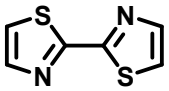

Synthesis of 2,2'-bithiazole (**11**)*:*
To an oven-dried 3-neck round-bottom flask cooled under N_2 was added Bu_4NBr. The flask was then vacuum-backfilled three times with N_2. 2-bromothiazole (2.60 g, 16 mmol, 1 equiv), Et(*i*-Pr)$_2$N (2.07 g, 16 mmol, 1 equiv.), and toluene (6 mL) were added to the flask. It was then degassed with N_2 for 30 minutes. $Pd(OAc)_2$ (359 mg, 1.6 mmol, 0.1 equiv.) was quickly added and the flask was heated at 105 °C overnight. The reaction mixture was cooled, H_2O (25 mL) was added, and it was extracted with $CHCl_3$. The combined organics were washed with brine and dried with Na_2SO_4. Purification was performed using column chromtagoraphy (20% EtOAc/hexanes). 587 mg, 43%. ^{1}H-NMR 400 MHz ($CDCl_3$): δ (ppm) 7.90 (d, J = 3.2 Hz, 2H), 7.44 (d, J = 3.2 Hz, 2H). Consistent with literature reports.[6]

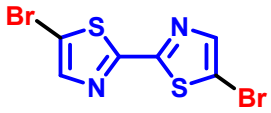

Synthesis of 5,5'-dibromo-2,2'-dithiazole (**12**)*:*
To an oven-dried 3-neck round-bottom flask cooled under N_2 was added 2,2'-dithiazole (**11**) (500 mg, 2.97 mmol, 1 equiv.) and anhydrous DMF (15 mL). NBS (2.14 g, 12 mmol, 4 equiv.) was added in one portion, and the reaction mixture was heated at 60 °C overnight. After cooling to room temperature, H_2O (25 mL) was added and the mixture was stirred for 15 minutes. The precipitate was filtered off, and it was then recrystallized with MeOH/$CHCl_3$. 571 mg, 59%. ^{1}H-NMR 400 MHz ($CDCl_3$): δ (ppm) 7.17 (s, 2H). Consistent with literature reports.[6]

3. ^{1}H-NMR for Compounds 2-12.

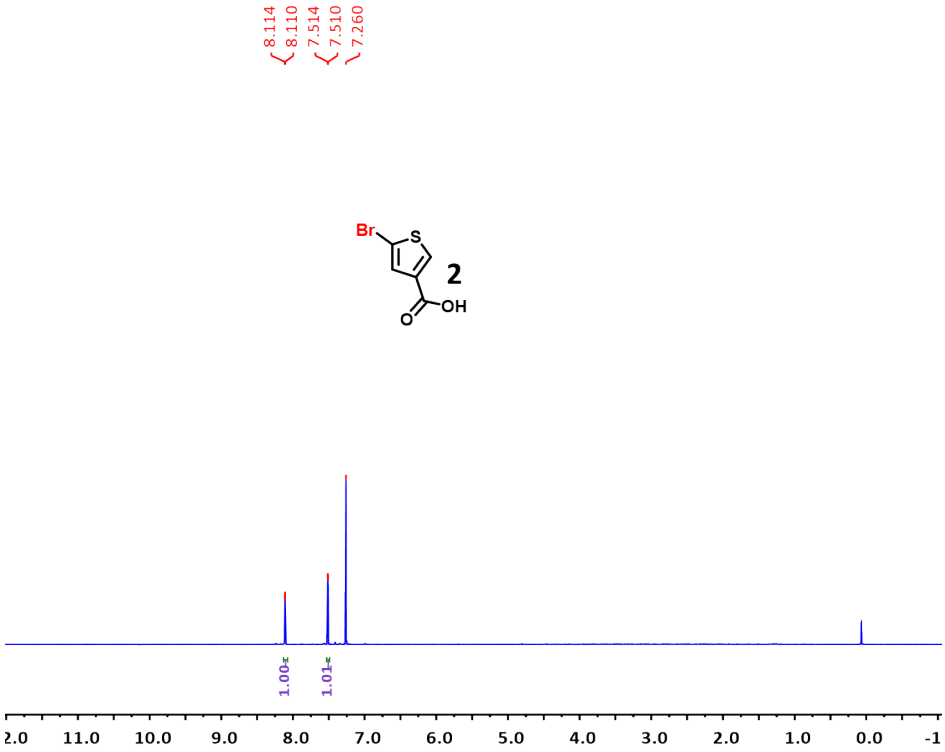

Figure S1. ^{1}H NMR of compound **2** in $CDCl_3$ at 25 °C and 400 MHz.

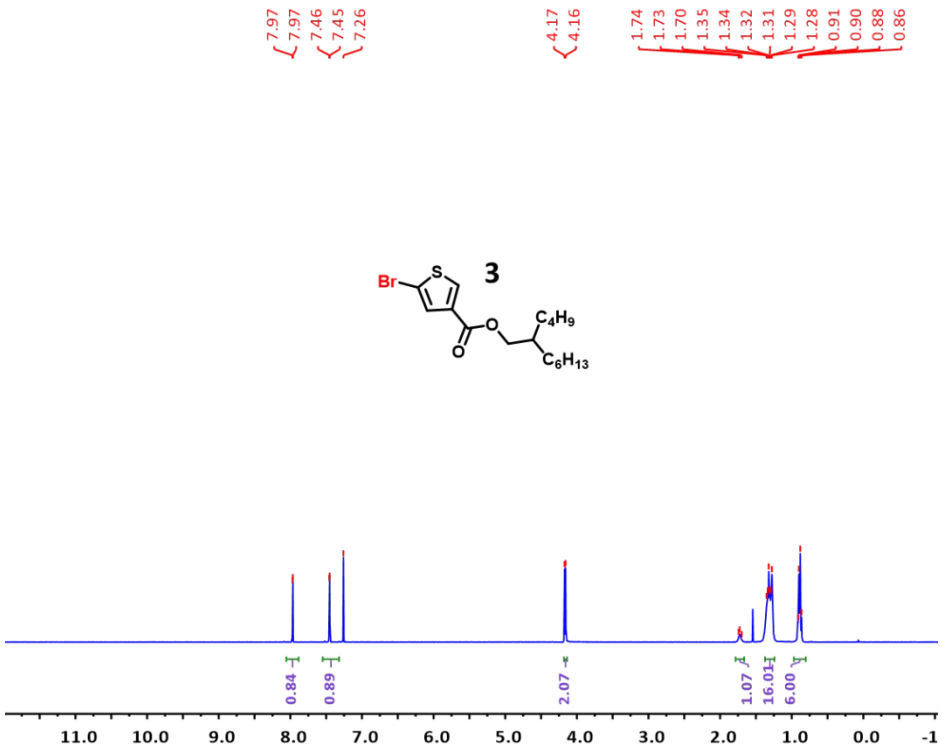

Figure S2. ^{1}H NMR of compound **3** in $CDCl_3$ at 25 °C and 400 MHz.

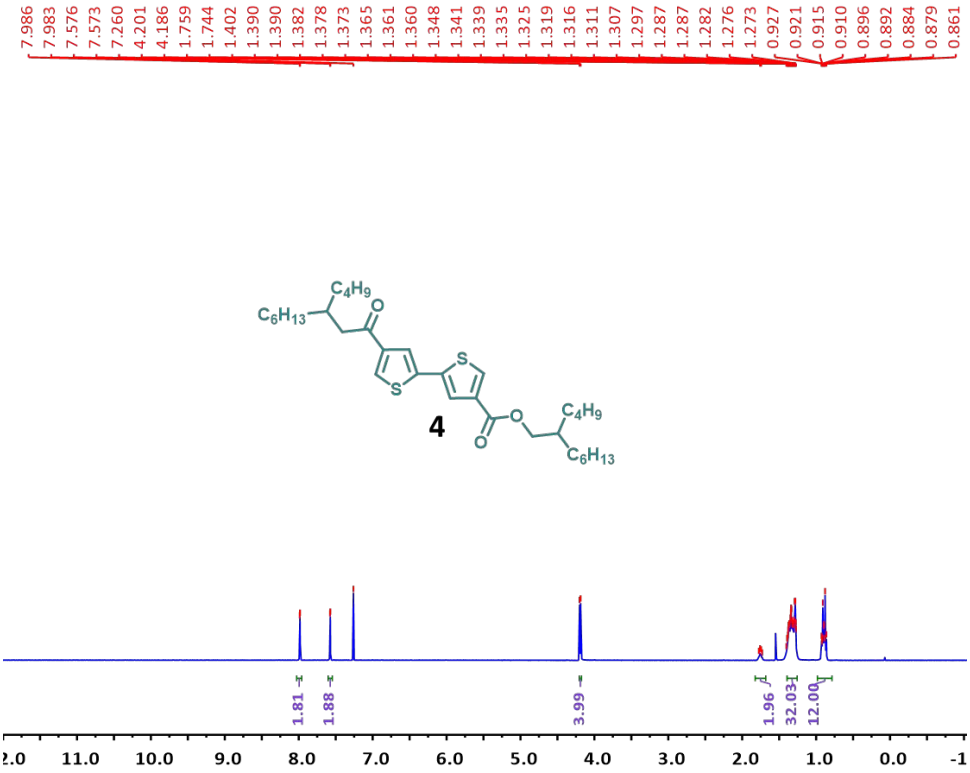

Figure S3. ^{1}H-NMR of Compound **4** in $CDCl_3$ at 25 °C and 400 MHz.

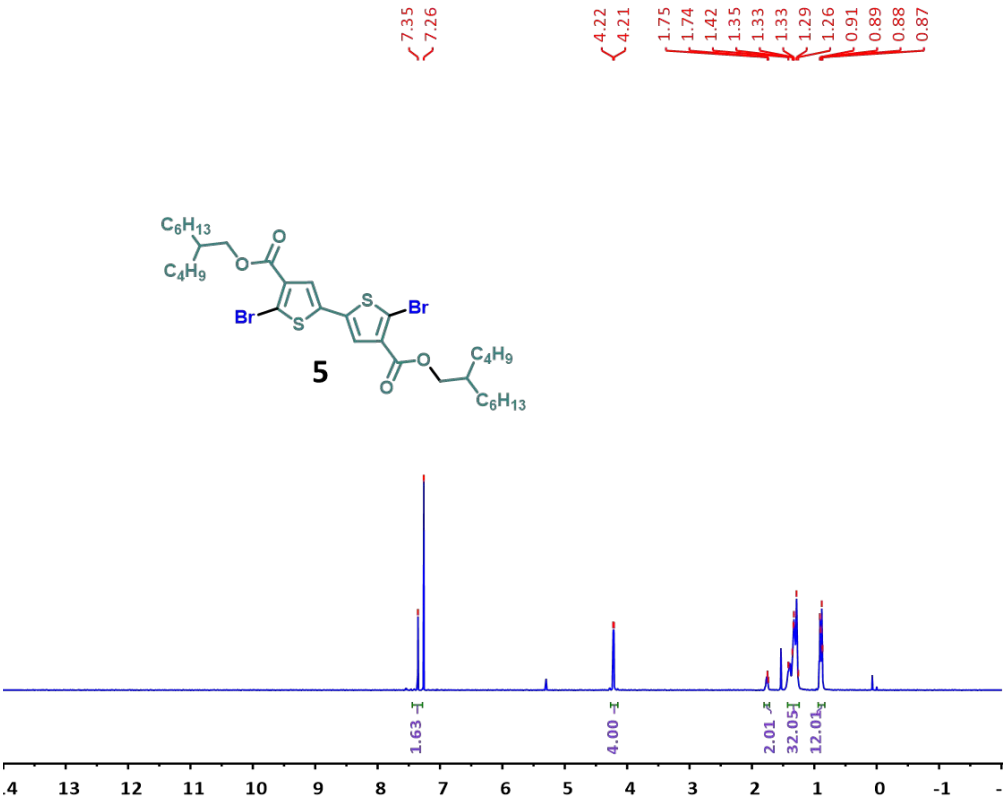

Figure S4. ^{1}H NMR of Compound **5** in $CDCl_3$ at 25 °C and 400 MHz.

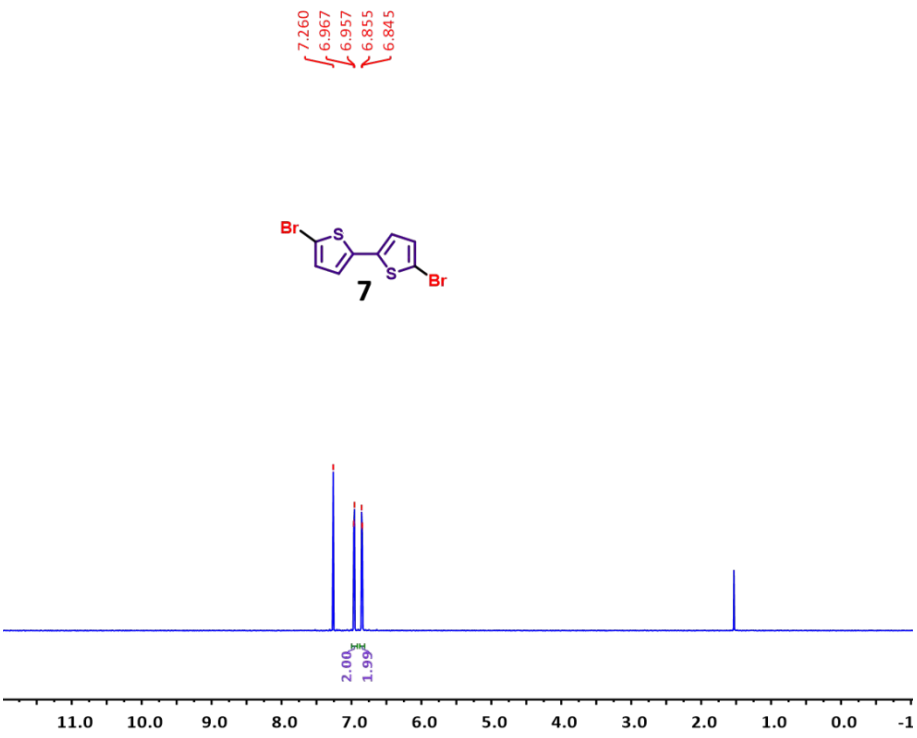

Figure S5. ^{1}H-NMR of monomer **7** in $CDCl_3$ at 25 °C and 400 MHz.

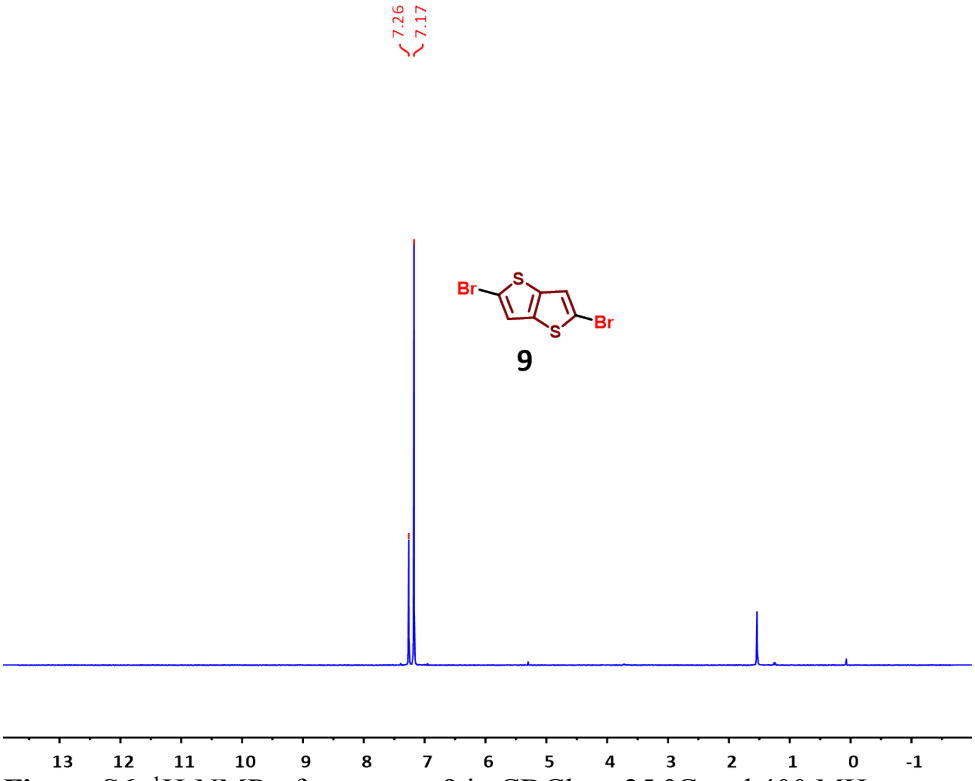

Figure S6. ^{1}H-NMR of monomer **9** in $CDCl_3$ at 25 °C and 400 MHz.

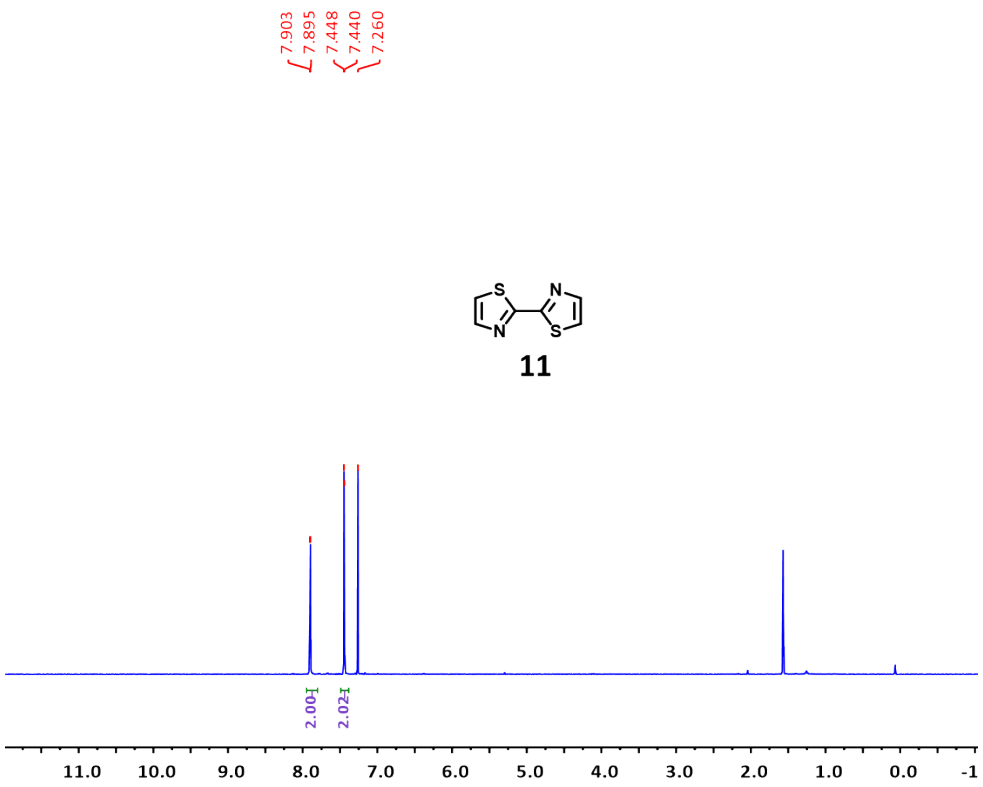

Figure S7. ^{1}H-NMR of compound **11** in $CDCl_3$ at 25 °C and 400 MHz.

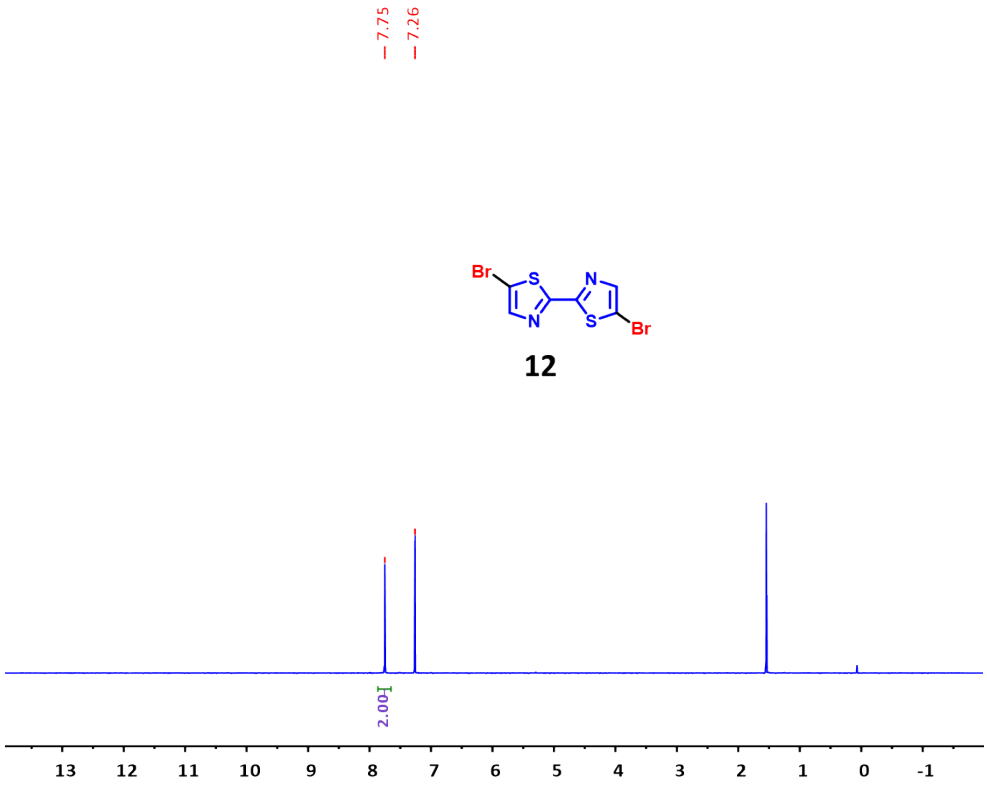

Figure S8. ^{1}H-NMR of monomer **12** in $CDCl_3$ at 25 °C and 400 MHz.

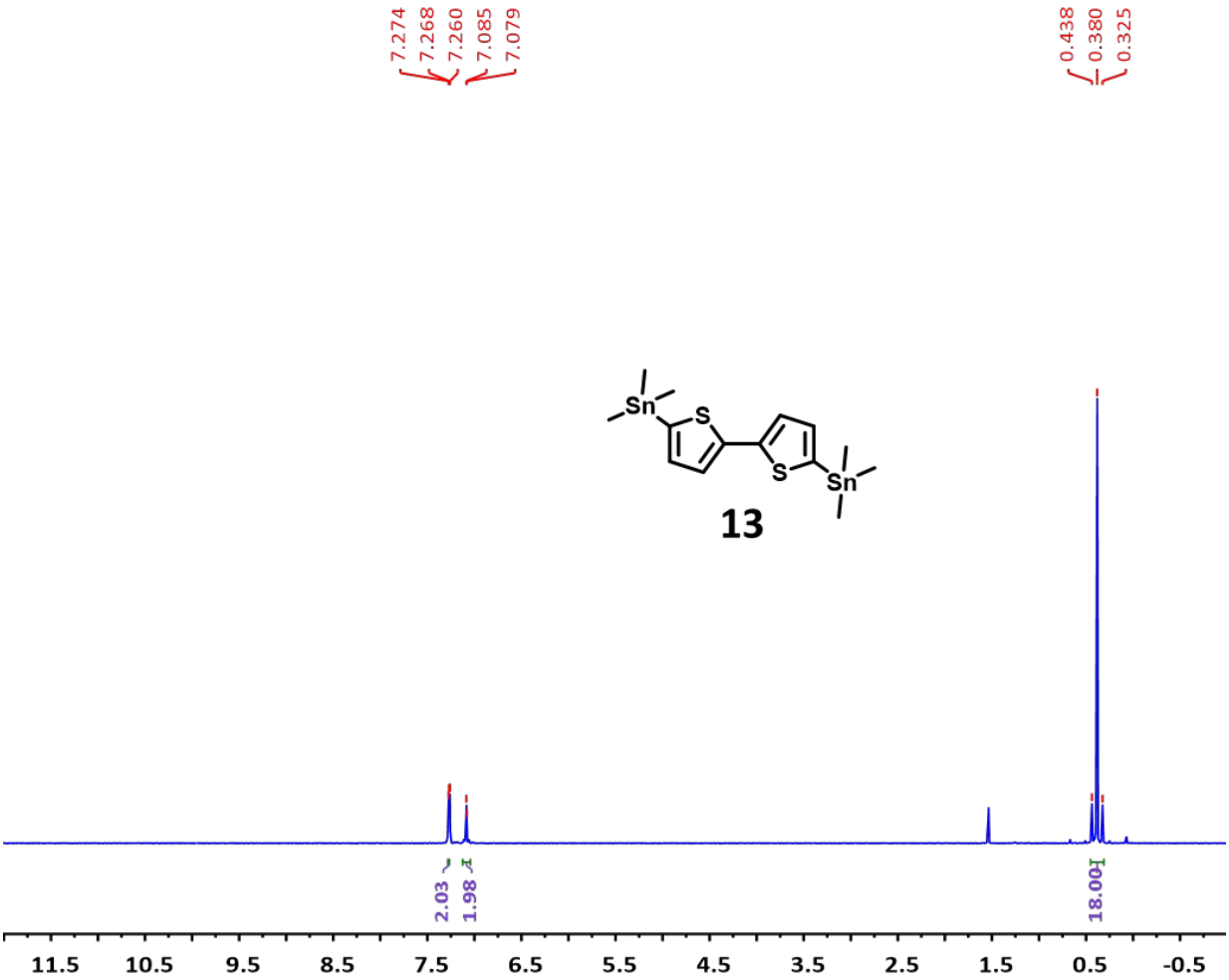

Figure S9. ^{1}H-NMR of monomer **13** in $CDCl_3$ at 25 °C and 500 MHz.

4. Polymer NMR

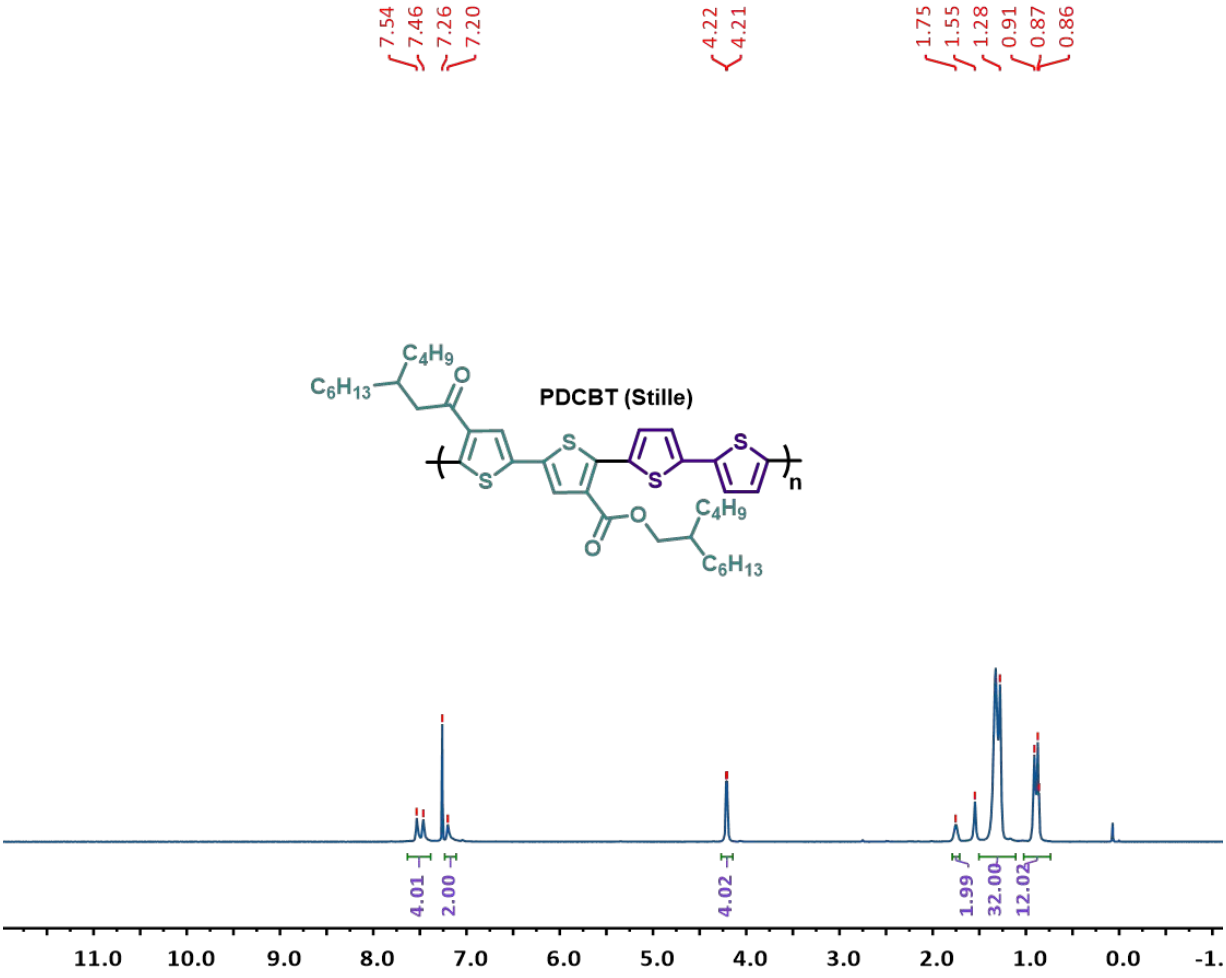

Figure S10. ^{1}H-NMR of PDCBT (Stille) collected in $CDCl_3$ at 25 °C and 500 MHz.

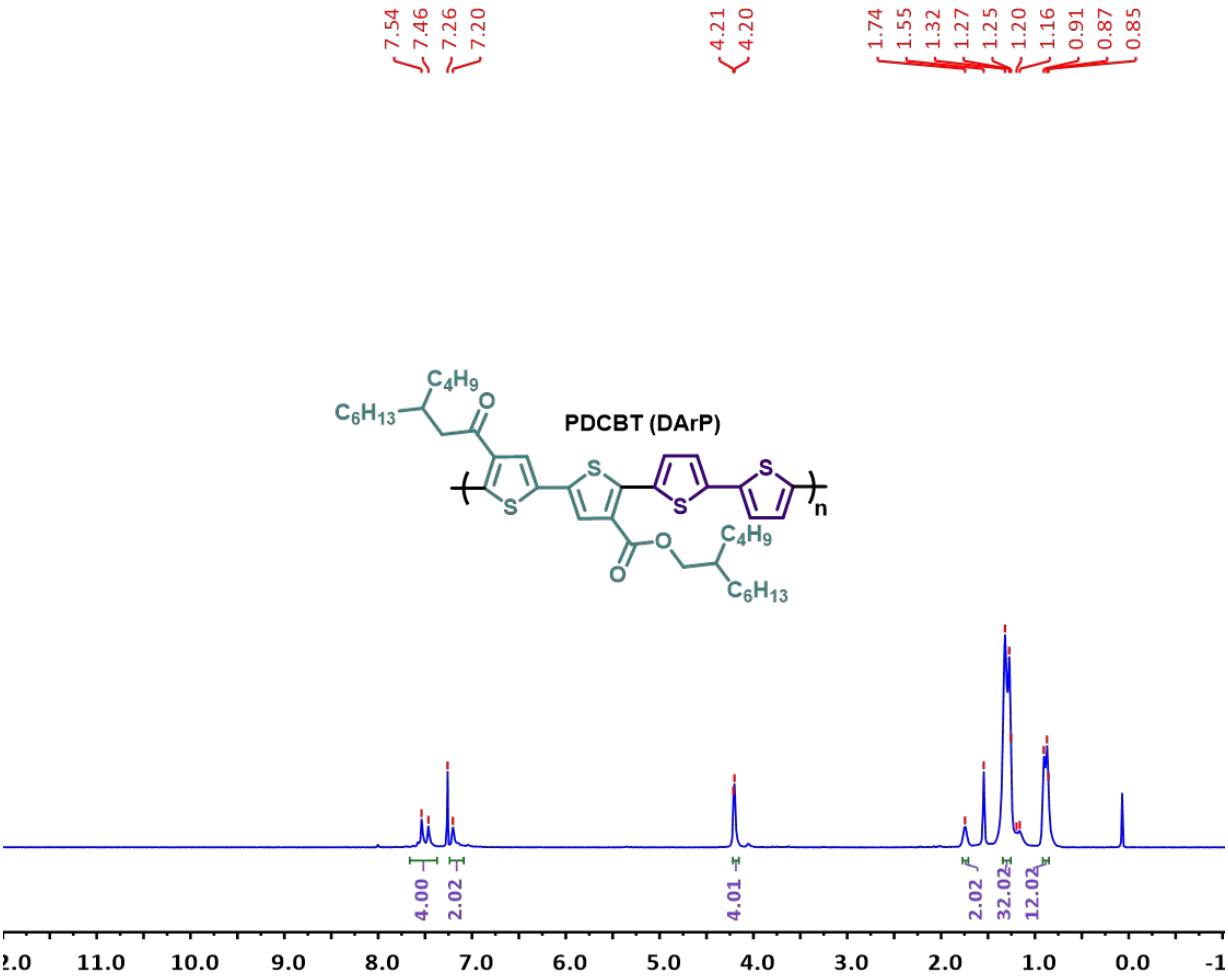

Figure S11. ^{1}H-NMR of PDCBT prepared via DArP (entry 3 of Table 1). Collected in $CDCl_3$ at 25 °C and 500 MHz.

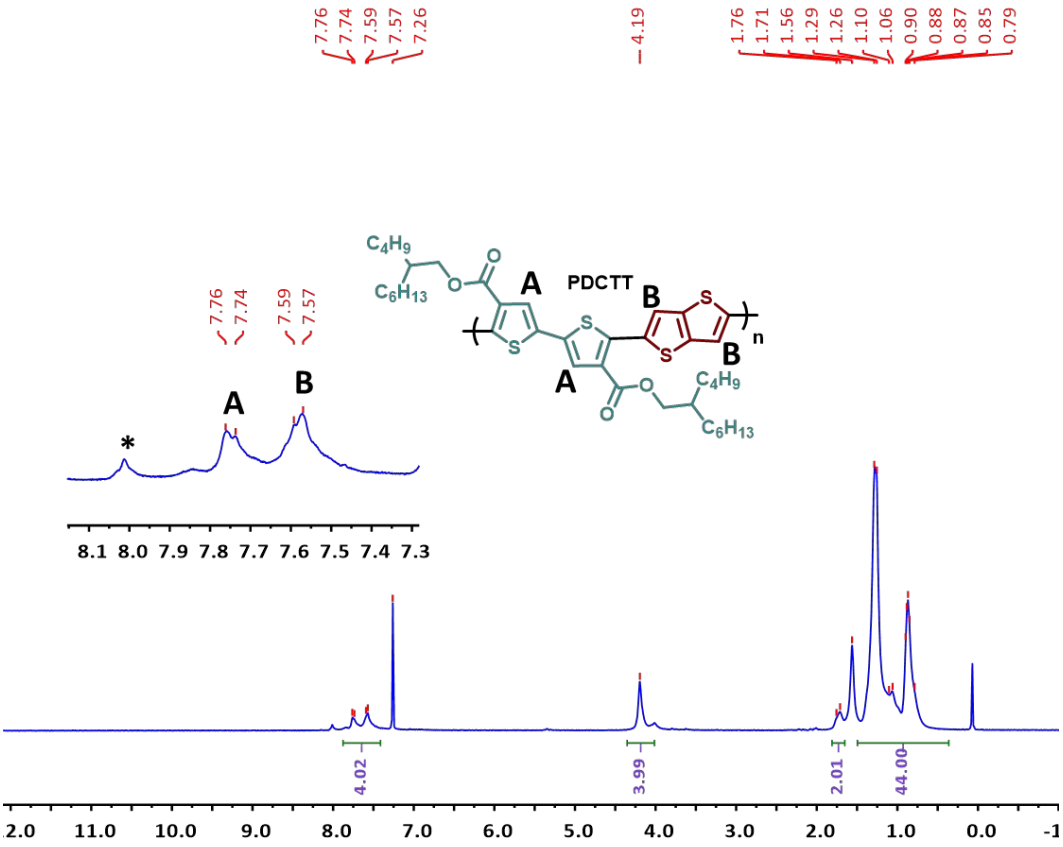

Figure S12. ^{1}H-NMR of PDCTT (entry 8 of Table 1) collected in $CDCl_3$ at 25 °C and 500 MHz. (*)Denotes potential end-group.

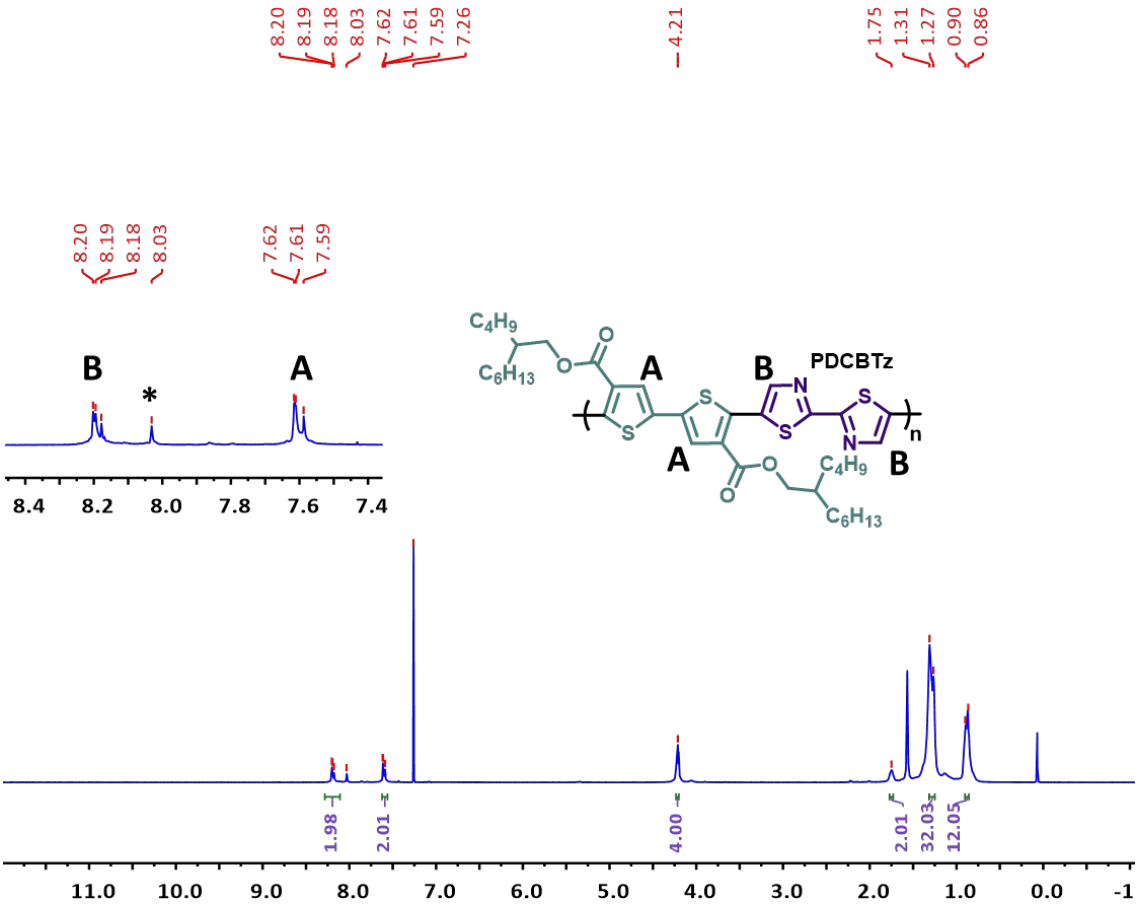

Figure S13. ^{1}H-NMR of PDCBTz (entry 9 of Table 1) collected in $CDCl_3$ at 25 C and 600 MHz. (*) Denotes potential end-group.

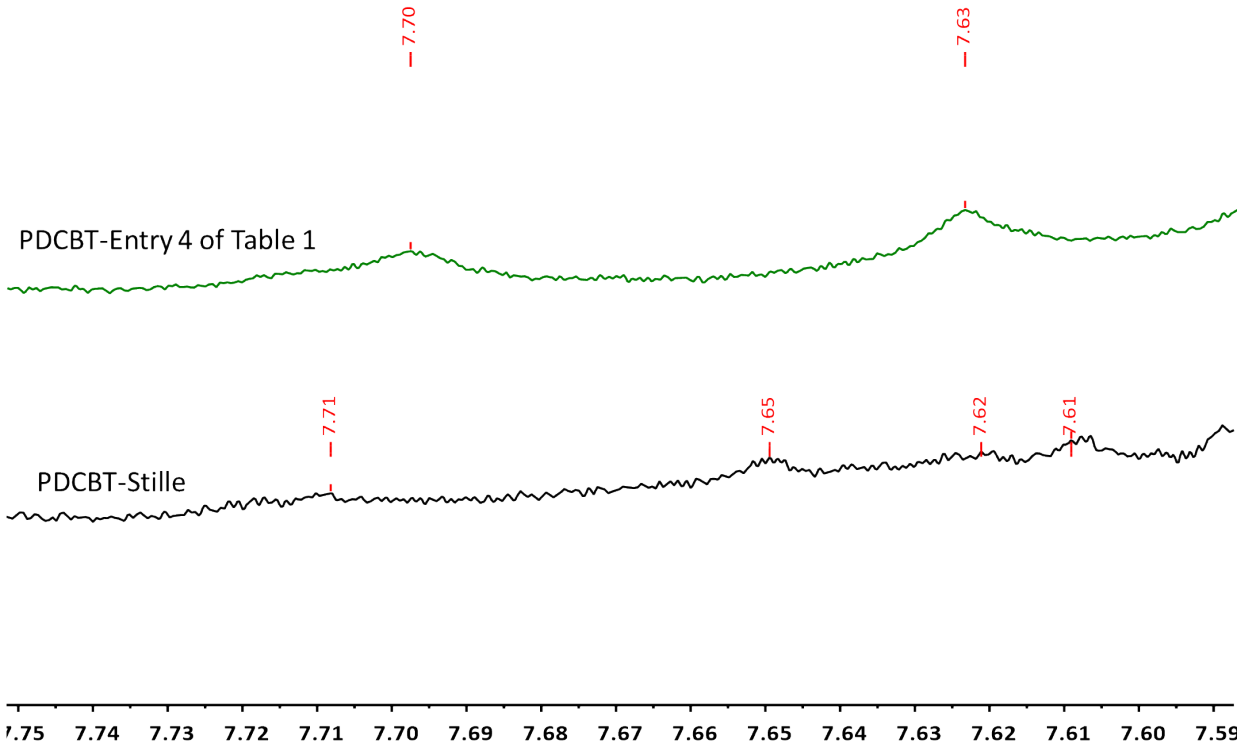

Figure S14. Expanded view of the region δ(ppm)7.75-7.55 in the ^{1}H-NMR spectra for PDCBT prepared by DArP (top) and Stille (bottom). Detailing what are likely penultimate protons for the respective DArP and Stille polymers.

5. Polymer GIXRD

Polymer	2θ (degrees)	d_{100} (Å)	Height	FWHM (degrees)	Crystallite size (nm)
PDCBT- Stille	4.250	20.7729	12801	0.531	14.96546
PDCBT-DArP	4.151	21.2673	2430	0.593	13.40035
PDCBTz	4.251	20.7714	5016	0.691	11.50024

6. GPC Traces

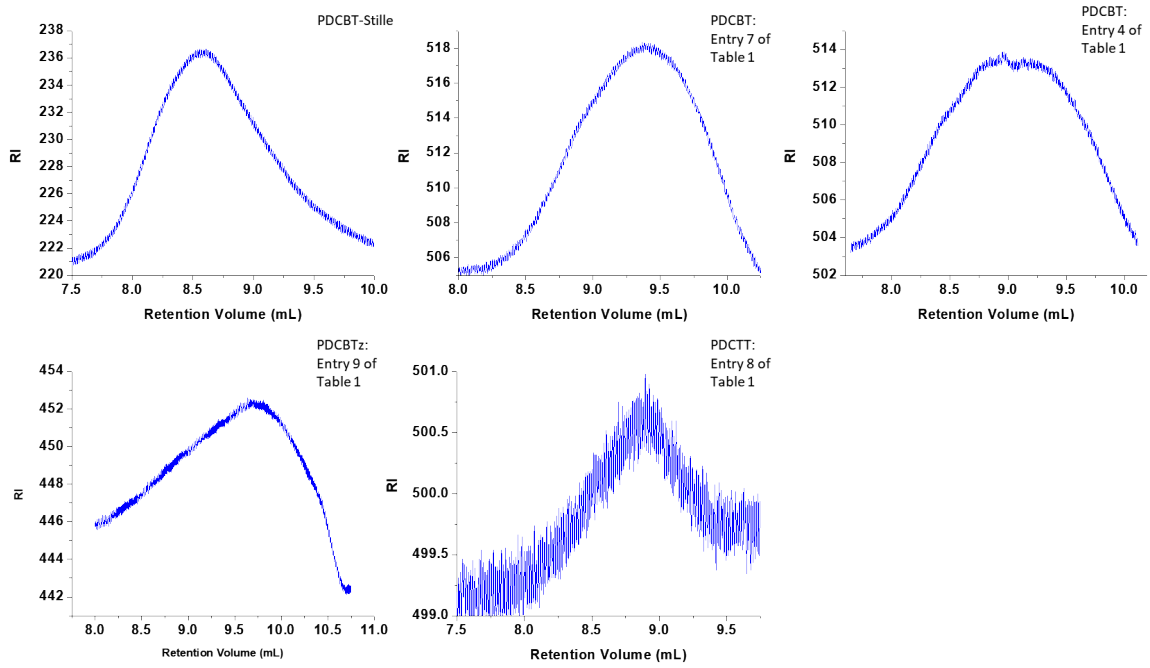

7. References

1 J. Choi, K.-H. Kim, H. Yu, C. Lee, H. Kang, I. Song, Y. Kim, J. H. Oh and B. J. Kim, *Chem. Mater.*, 2015, **27**, 5230–5237.
2 R. Heuvel, F. J. M. Colberts, M. M. Wienk and R. A. J. Janssen, *J. Mater. Chem. C*, 2018, **6**, 3731–3742.
3 M. Zhang, X. Guo, W. Ma, H. Ade and J. Hou, *Adv. Mater.*, 2014, **26**, 5880–5885.
4 L. G. Reuter, A. G. Bonn, A. C. Stückl, B. He, P. B. Pati, S. S. Zade and O. S. Wenger, *J. Phys. Chem. A*, 2012, **116**, 7345–7352.
5 Z. Yuan, Y. Xiao, Y. Yang and T. Xiong, *Macromolecules*, 2011, **44**, 1788–1791.
6 K. Oniwa, H. Kikuchi, T. Kanagasekaran, H. Shimotani, S. Ikeda, N. Asao, Y. Yamamoto, K. Tanigaki and T. Jin, *Chem. Commun.*, 2016, **52**, 4926–4929.